Author Manuscript

Author Manuscript

Author Manuscript

Author Manuscript

HHS Public Access

Author manuscript

Pflugers Arch. Author manuscript; available in PMC 2023 July 05.

Published in final edited form as:

Pflugers Arch. 2023 March ; 475(3): 323–341. doi:10.1007/s00424-022-02767-8.

Apolipoprotein L1 (APOL1) cation current in HEK-293 cells and in human podocytes

David H. Vandorpe[1,2], **John F. Heneghan**[1,#,@], **Joshua S. Waitzman**[1,2,#], **Gizelle M. McCarthy**[1,%], **Angelo Blasio**[1,%], **Jose M. Magraner**[1,@@], **Olivia G. Donovan**[1], **Lena B. Schaller**[1,^], **Shrijal S. Shah**[1,^^], **Balaji K. Subramanian**[1,2], **Cristian V. Riella**[1,2], **David J. Friedman**[1,2,3], **Martin R. Pollak**[1,2,3], **Seth L. Alper, MD-PhD**[1,2,3,*]

[1]Division of Nephrology and Department of Medicine, Beth Israel Deaconess Medical Center, Boston, MA 02215;

[2]Department of Medicine, Harvard Medical School, Boston, MA 02115;

[3]Broad Institute of Harvard and MIT, Cambridge, MA 02139

Abstract

[*]Correspondence to: Seth L. Alper, MD-PhD, Beth Israel Deaconess Medical Center RN380F, 99 Brookline Ave., Boston, MA 02215, salper@bidmc.harvard.edu.

[@],Current address: Department of Pathology, Brigham and Women's Hospital, Boston, MA 02215

[%],Current address: Vertex Pharmaceuticals, Boston, MA 02210

[@@],Current address: San Diego, CA

[^],Current address: Ludwig-Maximilians-Universitaet, 80336 Munich, Germany

[^^],Current Address: Chroma Medicine, Cambridge, MA 02142

Authors' contributions:

David H. Vandorpe, Beth Israel Deaconess Medical Center, Boston, MA, United States: conceived the project, performed experiments, analyzed results, prepared figures, wrote and revised the main manuscript text and reviewed the manuscript.

John F. Heneghan, Beth Israel Deaconess Medical Center, Boston, MA, United States: performed experiments, analyzed results and reviewed the manuscript.

Joshua S. Waitzman, Beth Israel Deaconess Medical Center, Boston, MA, United States: performed experiments, revised the main manuscript text and reviewed the manuscript.

Gizelle M. McCarthy, Beth Israel Deaconess Medical Center, Boston, MA, United States: performed experiments, prepared figures, analyzed results, revised the main manuscript text and reviewed the manuscript.

Angelo Blasio, Beth Israel Deaconess Medical Center, Boston, MA, United States: performed experiments, analyzed results, prepared figures and reviewed the manuscript.

Jose M. Magraner, Beth Israel Deaconess Medical Center, Boston, MA, United States: performed experiments.

Olivia G. Donovan, Beth Israel Deaconess Medical Center, Boston, MA, United States: performed experiments.

Lena B. Schaller, Beth Israel Deaconess Medical Center, Boston, MA, United States: performed experiments.

Shrijal S. Shah, Beth Israel Deaconess Medical Center, Boston, MA, United States: performed experiments, prepared figures and reviewed the manuscript.

Balaji K. Subramanian, Beth Israel Deaconess Medical Center, Boston, MA, United States: performed experiments, prepared figures and reviewed the manuscript.

Cristian V. Riella, Beth Israel Deaconess Medical Center, Boston, MA, United States: performed experiments, analyzed results and reviewed the manuscript.

David J. Friedman, Beth Israel Deaconess Medical Center, Boston, MA, United States: conceived the project, revised the main manuscript text and reviewed the manuscript.

Martin R. Pollak, Beth Israel Deaconess Medical Center, Boston, MA, United States: conceived the project, revised the main manuscript text and reviewed the manuscript.

Seth L. Alper, Beth Israel Deaconess Medical Center, Boston, MA, United States: conceived and oversaw the project, analyzed results, prepared figures, wrote and revised the main manuscript text, reviewed the manuscript.

[#],Equal contributions

Consent for publication: All authors have read the manuscript and consent to its publication.

Competing interests: Co-authors MRP and DJF are inventors on patents related to APOL1, hold equity in Apolo1bio, and have consulted for and received research support from Vertex.

Author Manuscript Author Manuscript Author Manuscript Author Manuscript

Two heterozygous missense variants (G1 and G2) of Apolipoprotein L1 (APOL1) found in individuals of recent African ancestry can attenuate the severity of infection by some forms of *Trypanosoma brucei*. However, these two variants within a broader African haplotype also increase the risk of kidney disease in Americans of African descent. Although overexpression of either variant G1 or G2 causes multiple pathogenic changes in cultured cells and transgenic mouse models, the mechanism(s) promoting kidney disease remain unclear.

Human serum APOL1 kills trypanosomes through its cation channel activity, and cation channel activity of recombinant APOL1 has been reconstituted in lipid bilayers and proteoliposomes. Although APOL1 overexpression increases whole cell cation currents in HEK-293 cells, the ion channel activity of APOL1 has not been assessed in glomerular podocytes, the major site of APOL1-associated kidney diseases.

We characterize APOL1-associated whole cell and on-cell cation currents in HEK-293 T-Rex cells and demonstrate partial inhibition of currents by anti-APOL antibodies. We detect in primary human podocytes a similar cation current inducible by interferon-γ (IFNγ) and sensitive to inhibition by anti-APOL antibody as well as by a fragment of *T. Brucei* Serum Resistance-Associated protein (SRA). CRISPR knockout of APOL1 in human primary podocytes abrogates the IFNγ-induced, antibodysensitive current.

Our novel characterization in HEK-293 cells of heterologous APOL1-associated cation conductance inhibited by anti-APOL antibody and our documentation in primary human glomerular podocytes of endogenous IFNγ-stimulated, APOL1-mediated, SRA and anti-APOL-sensitive ion channel activity together support APOL1-mediated channel activity as a therapeutic target for treatment of APOL1-associated kidney diseases.

Keywords

Focal Segmental Glomerulosclerosis; interferon-γ; serum resistance-associated; patch clamp; antibody

Introduction

Americans of West African descent face a risk of kidney disease 4-to-5-fold higher than experienced by those of European origin. Most of this increased risk has been traced to two missense variants of the human- and great ape-specific innate immune gene product, Apolipoprotein L1 (APOL1) [17,47]. The kidney disease risk variants, known as G1 and G2, are found only as part of an *APOL1* haplotype present in many African populations [26]. Heterozygosity for either G1 or G2 variants confers partial resistance to African sleeping sickness, trypanosomiasis mediated by the tsetse fly salivary gland parasites *Trypanosoma brucei gambiense, T. brucei brucei* and, more controversially, *T. brucei rhodesiense*. Evolutionary selection for this resistance to an endemic disease has led to expansion of the *APOL1* G1 and G2 variants to high allele frequency among African populations [35]. *APOL1* risk variant allele frequencies exceed 50–60% in areas of West Africa [46], with allele frequencies among African-Americans of ~23% (G1) and ~14% (G2). However, homozygosity or compound heterozygosity for the G1 and G2 variants of *APOL1* predisposes carriers to increased risk of acute and/or chronic kidney disease [17].

Author Manuscript Author Manuscript Author Manuscript Author Manuscript

Among carriers of two *APOL1* risk alleles, ~13–15% will develop end-stage renal disease during their lifetimes [16]. These individuals experience increased risks of 7–10 fold for hypertension-associated kidney disease, 17-fold for focal segmental glomerular sclerosis (FSGS, OMIM phenotype 612551), ~30–90-fold for Human Immunodeficiency Virus (HIV)-nephropathy and elevated risks of lupus nephropathy, membranous nephropathy, pre-eclampsia, transplant nephropathy and sickle nephropathy [16,56]. Multiple mechanisms have been proposed to explain how APOL1 risk variants predispose to this wide range of kidney diseases [16,4,15,25], including endoplasmic reticulum stress, cytoskeletal perturbations, lipotoxicity, altered metabolic state, mitochondrial damage, cGAS-STING pathway activation, and plasmalemmal ion channel gain-of-function. Most of these studies derive from experiments with immortalized epithelial cell lines.

The ion channel gain-of-function phenotype has been studied in several systems of heterologous expression and reconstitution [32]. APOL1-associated cation channel activity has been demonstrated in *Xenopus laevis* oocytes [21] and in HEK-293 cells [33,30]. APOL1 expression-associated increased permeability to Ca^{2+} has been documented in *Xenopus* oocytes [21], planar lipid bilayer, HEK-293 cells and HeLa cells [18]. Recombinant APOL1 proteins have been shown to be both necessary and sufficient to mediate cation currents across planar lipid bilayers [45,18,41,40,28]. APOL1-mediated cation permeability has been revealed by reconstitution of similarly purified APOL1 into proteoliposomes, using ionophore-regulated quenching of ion-selective fluorescent dyes [6,7]. APOL1 has also been shown to induce permeabilization of both lysosomal and mitochondrial membranes in trypanosomes [49]. However, ion channel activity of APOL1 has not yet been reported in glomerular podocytes, the cell type in which APOL1 risk variant-induced toxicity is believed to cause acute FSGS and to contribute to multiple forms of chronic kidney disease. Detection of APOL1-mediated channel activity in intact cells has been complicated by variable background channel activity, by APOL1 expression-associated cytotoxicity [30] and by the lack of a small molecule pharmacological signature characteristic of APOL1-mediated channel activity.

The above cell biological and biochemical studies have been complemented by investigation of transgenic [3] [5]) and BAC/fosmid mouse models of APOL1 kidney disease [31,1,27]. In these models, high interferon states of the types associated with viral infection have been shown to contribute to APOL1 risk variant-associated glomerular pathology resembling FSGS [34,29].

Here, we extend the characterization of APOL1-associated cation channel activity in doxycycline-inducible HEK-293 T-Rex cells, showing that G1-associated whole cell currents are of higher magnitude than G0-associated currents. We find that two commercially available (oligospecific) anti-APOL1 antibodies inhibit APOL1-associated whole cell and unitary currents. We then detect and characterize IFNγ-induced APOL1-associated currents in whole cell and unitary recordings from primary human glomerular podocytes. We demonstrate preserved sensitivity of these podocyte currents to blockade by extracellular anti-APOL1 antibody and (for APOL1 G0-mediated currents) to blockade by extracellulr exposure to trypanosomal Serum-resistance Associated protein (SRA). We then show loss of these IFNγ-induced, SRA-sensitive currents in primary human podocytes

Author Manuscript Author Manuscript Author Manuscript Author Manuscript

subjected to CRISPR-Cas9 knockout of endogenous APOL1. We conclude that IFNγ-stimulated cation currents in primary cultured human glomerular podocytes are mediated in large part by endogenous APOL1.

Materials and Methods

DNA constructs

APOL1 (OMIM gene locus #603743) variants G0 (African Common, or AfCom), G1 (rs73885319, rs60910145) and G2 cDNAs (rs71785313) were as previously described [10,26,33,42,57]. (See Shah et al.[42] for complete APOL1 cDNA sequences). APOL1 mammalian expression vectors were of naturally occuring haplotypes [26]. APOL1 has OMIM gene locus #603743). cDNA encoding aa 24–267 of *T. brucei rhodesiense* Serum Resistance-Associated [8] was the gift of Mark Carrington, Univ. of Cambridge.

Cell lines

HEK-293 T-Rex cells were from Thermo-Fisher (Waltham, MA). Coverslips or wells were coated in 0.1 mg/ml polylysine and air-dried in the hood prior to cell plating. Attached cells at 50–80% confluency were transfected with 0.5 μg plasmid cDNA and 1 μl each of Lipofectamine P3000 and Lipofectamine reagent (ThermoFisher) per well in OptiMEM (Life Technologies) as per manufacturer's instructions. Stable, tetracycline-inducible, transgenic HEK T-Rex-293 cell lines with human APOL1 G0, G1, or G2 integrated at a defined locus [10,26,33,42,57] were grown in Dulbecco's modified Eagle's medium (DMEM, Corning) supplemented with 10% tetracycline system-approved fetal bovine serum (Atlanta Biologicals), 0.2 mg/ml zeocin, 2 ug/ml blasticidin and 1% antibiotic-antimycotic at 37°C and 5% CO_2. Cells were induced to overexpress APOL1 by 6–24 h exposure to 50 ng/ml doxycycline, as indicated. For electrophysiological experiments, cells were induced 6 h with 50 ng/ml doxycycline, and subjected to electrical recording on the same day.

Human primary podocytes (Celprogen, Torrance, CA) were grown per supplier's recommendations in Celprogen human podocyte primary cell culture complete growth medium and subcultured every 48 h on Celprogen podocyte cell culture extracellular matrix. Celprogen podocytes thus maintained have been documented to express podocyte markers nephrin, podocin, synaptopodin, CD2AP, PAX2 and WT1 through at least passage 6 [50,37] and (Chun J. and Riella C., pers. comm.). The APOL1 genotype of Celprogen primary podocytes was confirmed by RT-PCR and DNA sequencing as G0/G0. Podocytes were induced to express endogenous APOL1 by exposure to 10 ng/ml IFNγ for 18–24 h.

Cells were validated as free of Mycoplasma contamination.

Antibodies

Rabbit polyclonal anti-APOL1 antibody raised against an N-terminal GST-fusion protein containing APOL1 residues 1–238 (numbered according to NP_003652, APOL1 transcript variant 1) was from Proteintech (Rosemont, IL; cat. # 11486–2-AP). Rabbit polyclonal anti-APOL1 C-terminal region raised against recombinant APOL1 aa 262–387 was from Sigma

Author Manuscript Author Manuscript Author Manuscript Author Manuscript

(St. Louis, MO; cat # HPA018885). The Proteintech anti-APOL1 antibody has been more recently shown to cross-react with human APOL2 and APOL3 as assayed by immunoblot and immunofluorescence microscopy, whereas the Sigma anti-APOL1 antibody was shown to cross-react only with human APOL2 in the same detection modalities [39]. Rabbit monoclonal antibody to human NA,K-ATPase α subunit was from Abcam (cat. # ab76020). Sheep polyclonal antibody to human nephrin was from R&D Systems (cat. AF4269). Rabbit polyclonal antibody to human WT1 was from Proteintech (12609–1-AP). Rabbit polyclonal affinity-isolated antibody to human podocin was from Sigma (P0372). Nonspecific rabbit IgG was from Bethyl Laboratories (Montgomery, TX) or from Sigma (St. Louis, MO).

Immunoblot

Cells washed with ice-cold PBS were lysed in 1% NP-40 lysis buffer (50 mM Tris-HCl [pH 7.4], 150 mM NaCl, 5 mM EDTA, 1% NP-40 (Boston Bioproducts) supplemented with complete™, Mini, EDTA-free Protease Inhibitor Cocktail (Sigma) and PhosSTOP (Sigma). Lysates cleared by 10 min centrifugation at 16,000 × g and 4°C were boiled 5 min in SDS sample buffer with β-mercaptoethanol and separated by SDS-PAGE (Bio-Rad). Precision Plus dual color molecular size standards (Bio-Rad) were run in a separate lane. Proteins transferred to PVDF membranes were blocked in 5% (w/v) skim milk in tris buffered saline with 0.05% tween for 1 h, then incubated overnight at 4°C with primary antibody (1:1000). Immunoblots were washed with TBST and incubated with appropriate horseradish peroxidase-conjugated secondary antibodies (Santa Cruz Biotechnologies, 1:2500 or (for Fig. 7) 1:4000) visualized by ECL chemiluminescence (SuperSignal™ West Dura or Femto kit; Life Technologies) and imaged (Proteinsimple FluorChem E or R; Bio-Techne). Band intensity was quantitated by densitometric analysis using ImageJ (version 1.47).

Confocal Immunofluorescence microscopy

HEK-293 T-Rex cells grown on polylysine (Fig 1C) collagen-coated glass coverslips and treated without or with 100 ng doxycycline for 6–24 h were washed 3x, fixed 20 min with 4% paraformaldehyde and quenched with 50 mM ammonium chloride, but not detergent-permeabilized. Fixed, non-permeabilized cells were blocked with 0.2% gelatin in PBS followed by overnight incubation with primary antibodies to APOL1 (Proteintech mouse monoclonal, 1:100) and to Na,K-ATPase α subunit (Abcam rabbit monoclonal, 1:500). Rinsed cells were then incubated 1 hr with Alexa-Fluor 488- or 555-labelled secondary antibodies (ThermoFisher Scientific). Fixed, stained cells were washed, mounted with ProLong® Gold antifade reagent with or without DAPI (ThermoFisher Scientific). Confocal images were acquired by LSM 880 laser scanning microscope (Zeiss) with a 63X oil lens, NA 1.4, or 20x water lens.

Human primary podocytes (Celprogen, passage 9) plated on collagen-coated coverslips in 24 well plates were treated 18–24 h without or with IFNγ (10 ng/ml). Washed cells were fixed but not permeabilized as above. Fixed non-permeabilized cells were incubated 2 h at room temperature with primary anti-APOL1 antibody (Proteintech polyclonal, 1:250) and anti-Na,K-ATPase α subunit (Abcam monoclonal, 1:250). Rinsed cells were further incubated 1 h at room temperature with secondary Alexa-555-coupled rabbit anti-mouse

Author Manuscript Author Manuscript Author Manuscript Author Manuscript

Ig and with secondary Alexa-488-coupled goat anti-rabbit Ig (both at 1:500). Post-staining processing was as for T-Rex cells in the preceding paragraph.

SRA polypeptide expression

cDNA encoding the N-terminal fragment of SRA (aa 24–267) was subcloned into the pGEX-4T1 expression vector. Ligation products were transformed into *E coli* BL21(DE3) cells (EMD) and DNA sequence integrity confirmed. DNA quantitation was performed by Nanodrop spectrometer (Thermo-Fisher). Recombinant SRA polypeptide was generated as previously described [43] with modifications, and aliquots were stored at −80° C in 150 mM NaCl, 5 mM DTT, 10 mM reduced glutathione, and 50 mM Tris HCl, pH 8, until use. The SRA polypeptide was applied to cultured podocytes at 1.5 μM (or ~6 times IC_{50}) in the pipette solution, based on a surface plasmon resonance-determined IC_{50} of 277 nM for APOL1 binding to SRA aa 24–267 [58] (see below).

CRISPR knockout of APOL1 in primary human podocytes

An APOL1 sgRNA 5'- GTGCAACAAAACGTTCCAAG-3' ("guide 4"), was used to target the 5'-end of APOL1 exon 5 encoding aa 34–39, a region without nucleotide homology to APOL2 or APOL6. Preliminary experiments established sgRNA guide 4 as the most effective among the four APOL1 sgRNAs available in the Brunello sgRNA library (Addgene, see [13]). sgRNA guide 4 was subcloned into pLentiCRISPRv2 (https://media.addgene.org/cms/filer_public/6d/d8/6dd83407-3b07-47db8adb-4fada30bde8a/zhang-lab-general-cloning-protocol-targetsequencing_1.pdf) (Addgene). HEK-293T cells were transfected with pLentiCRISPRV2-EV or pLentiCRISPRv2-guide 4, plasmid psPax2 (Addgene), and plasmid pMD2.G (Addgene) in a 10:7.5:3 ratio using Lipofectamine 2000 (ThermoFisher). Supernatants were collected 2 days later and filtered through a 45 μM filter. 1 mL of virus-containing medium and 1 mL of fresh medium were added to Celprogen primary human podocytes in culture. On day 3, viral supernatant was again collected, filtered, and added with fresh medium to the podocytes. On day 4, selection was imposed with 2 μg/mL puromycin. After achieving confluency, podocytes were passaged at near-limiting dilution into 96-well plates (estimated 0.5 cells/well) in 50% conditioned media. Following appearance of clonal/oligoclonal colonies on the 96 well plate, individual colonies were passaged onto wells of a 24-well plate. The wells of the 24-well plate were then passaged in parallel onto wells of a 6-well plate for subsequent expansion onto 10 cm dishes and preservation in liquid nitrogen, and onto wells of a 12-well plate for characterization. Three putative knockout clonal lines from the 12-well plate were treated 24 h without or with interferon (10 ng/mL) and then evaluated for APOL1 expression by immunoblot and immunofluorescence microscopy.

Mammalian Cell Electrophysiology methods

For conventional whole cell patch clamp experiments, patch pipettes were pulled (Sutter Flaming-Brown P97 puller, Sutter, Novato, CA) from borosilicate glass capillaries to tip resistance of 1–3 MΩ when filled with pipette solution. Pipette tips were fire-polished by microforge (Narashige) before use. Cells plated on 5 mm coverslips were placed in a 200 μL open perfusion chamber (Warner Instruments, Hamden, CT) mounted on an inverted microscope and superfused at 3 ml/min with bath solution containing (in mM): 140 NaCl, 4

Author Manuscript Author Manuscript Author Manuscript Author Manuscript

KCl, 1 $CaCl_2$, 1 $MgCl_2$, 10 Hepes, pH 7.4. Pipette solution was (in mM): 140 KCl, 4 NaCl, 5 EGTA, 1 $CaCl_2$, 1 $MgCl_2$, 1 ATP, 5 Hepes, pH 7.4.

Whole cell patch clamp currents were recorded at room temperature (Axopatch 200B, Molecular Devices, Sunnyvale, CA) and digitized with a 1550B AD/DA board (Molecular Devices). Holding potential was −60 mV. For HEK-293 T-Rex cells, command potentials were stepped from −100 to +80 mV at 20 mV intervals, with pulse durations of 100 ms, followed by return to holding potential, using the Clampex subroutine of PCLAMP10. The pulse protocol was repeated every 10 sec until achievement of steady state, usually within 2–3 min. Resulting currents were analyzed with Clampfit. In experiments with antibody exposure, the pulse protocol was applied during a baseline (control) period, followed by a stop-flow period in the presence of added 2 μg/ml antibody (Anti-APOL1, Sigma or Proteintech; nonspecific rabbit IgG, Bethyl) until achievement of new steady-state current, followed in turn by resumption of flow to wash out antibody.

Whole cell patch clamp currents in human primary podocytes (Celprogen) were recorded with an Axopatch 200B amplifier using the Clampex subroutine of pClamp11 (Molecular Devices), applying a 500-ms ramp protocol from +100 to −100 mV, repeated every 10 s for the duration of the experiment [44]. The bath reference electrode was a silver chloride wire with a 3 M KCl agar bridge. Data were filtered at 500 Hz, digitized at 10 kHz by Clampex, and analyzed offline by Clampfit subroutine (pClamp11). Holding potentials in whole-cell patch clamp experiments were expressed as V_m, the pipette potential. The ramp current measured at −60 mV was chosen to report whole-cell conductance.

On-cell patch clamp currents from human primary podocytes were recorded at room temperature (Axopatch 200A amplifier, Molecular Devices) with symmetric bath and pipette solutions containing (in mM) 140 NaCl, 4 KCl, 1 $CaCl_2$, 1 $MgCl_2$, and 10 HEPES, pH 7.4. For current-voltage (I-V) relationships in Clampex (Pclamp11), the real-time control window in gap-free mode recorded current traces of 10–30 s duration at holding potentials ranging from −100 to +100 mV in 25 mV increments. Bath reference electrode was a silver chloride wire with a 3 M KCl agar bridge to minimize liquid junction potentials. Data were filtered at 500 Hz, digitized at 2 kHz by Clampex, and analyzed offline by Clampfit (Pclamp10). Holding potentials were usually expressed as −Vp, the negative of the pipette potential.

In experiments testing the effects of anti-APOL antibody and SRA on unitary currents, antibody or SRA were included in the pipette solution.

Statistical Analysis

Normally distributed data were analyzed by two-way student t-test (for comparison of two datasets) or by ANOVA with Bonferroni post-hoc test (for comparison of multiple datasets). Non-normally distributed data were analyzed by Kruskal-Wallis ANOVA or by Mann-Whitney test. Tests were performed by SigmaPlot 11.0 or 14.0 (Systat, San Jose, CA) or (for Fig. 1B) by Prism 9.0 (GraphPad, San Diego, CA).

Author Manuscript Author Manuscript Author Manuscript Author Manuscript

Results

APOL1 G1-associated currents in HEK-293 T-Rex cells are of higher magnitude than those associated with APOL1 G0.

HEK-293 T-Rex cells were engineered to allow inducible overexpression of human APOL1 variants. Cells were studied after 6 or 10 h doxycycline induction to minimize APOL1 expression-associated cytotoxicity [33]. The “African common” (AfCom) haplotype of APOL1 G0 encodes Lys150, whereas the African kidney risk haplotypes of APOL1 G1 (Ser342Gly/Ile384Met) and G2 (ΔAsn388Tyr389) encode Glu150 [26]. The immunoblot of Fig. 1A shows 6 h doxycycline-induced APOL1 expression in cells transformed with APOL1 AfCom form G0 and with APOL1 renal risk variants G1 and G2. Fig. 1B presents the ratio of APOL1 band intensity to that of vinculin (as load control) after 10 h induction by doxycycline, showing comparable polypeptide accumulation of AfCom variant APOL1 G0 and African variants G1 and G2.

To document peripheral cell membrane localization of induced APOL1 polypeptides, we fixed cells with 4% paraformaldehyde after 10 h doxycycline induction of APOL1, at which time cytotoxicity remained minimal. Immunostaining was performed without prior detergent permeabilization of the fixed cells. As shown in Fig. 1C, all cells expressed Na,K-ATPase in a plasmalemmal pattern. Cells expressing APOL1 G0, G1, and G2 all showed APOL1 in a plasmalemmal pattern resembling that of Na,K-ATPase, whereas cells harboring the empty vector (EV) revealed no APOL1 staining. Fixed APOL1-expressing cells permeabilized with detergent revealed intracellular localization of all three APOL1 isoforms (not shown) [42,10,33], in addition to the peripheral membrane localization of Fig. 1C. These data are consistent with previous reports of detection of plasmalemmal localization of APOL1 in conditions of heterologous overexpression [18,39].

APOL1-associated currents in HEK-293 T-Rex cells are inhibited by acid pH, Zn^{2+} and Gd^{3+}.

The plasmalemmal staining pattern of APOL1 suggested that APOL1-associated current should be detectable by patch clamp. We recorded whole cell cation currents from cells induced to express APOL1 G0, G1 or G2. The current-voltage (I-V) curve of Fig. 2A shows that G1- and G2-associated capacitance-normalized currents were ~2.5-fold larger in magnitude than those recorded in G0-expressing cells, whereas current magnitude in EV-transduced cells was much lower.

Consistent with APOL1-associated current properties in *Xenopus* oocytes [21], in lipid bilayer [45], in reconstituted proteoliposomes [7], and in previous reports in HEK-293 cells [30,18], whole cell G1-associated currents at pH 7.4 were greatly reduced upon bath transition to pH 6.0 (Fig. 2B). APOL1 G1-associated whole cell current in HEK-293 T-Rex cells was also sensitive to inhibition by μM concentrations of Zn^{2+} (Fig. 2C). Consistent with our previous studies of APOL1-associated currents and $^{45}Ca^{2+}$ influx into *Xenopus* oocytes [21], whole cell G1-associated current in T-Rex cells was inhibited by 1 mM Gd^{3+} (Fig. 2D). Inhibition by 100 μM ruthenium red trended towards significance (not shown).

Author Manuscript Author Manuscript Author Manuscript Author Manuscript

APOL1-associated currents in HEK-293 T-Rex cells exhibit preferential cation selectivity.

Although originally reported to be partially anion-selective, more recent reports of currents mediated by purified E. coli-expressed APOL1 polypeptide reconstituted into lipid bilayer [45] or reconstituted into proteoliposomes subjected to fluorescence quench measurements of ion flux [7,6] have concluded that APOL1 shows preferential cation selectivity at neutral pH. Additional experiments have documented Ca^{2+} permeability of APOL1 [21,18]. The near-zero reversal potentials of currents recorded in cells expressing APOL1 G0, G1, and G2 (Fig. 2A) were consistent with nonspecific cation selectivity of APOL1-associated current (with possible contribution of endogenous chloride conductance). Also consistent with a nonspecific cation current mediated by APOL1 G1 was its abrogation by bath substitution of NaCl with N-methyl-D-glucamine chloride (not shown).

To further explore cation selectivity of APOL1-associated currents, we conducted dilution potential experiments with HEK-293 T-Rex cells induced to express APOL1 G0 or APOL1 G1. Whole cell currents were recorded first in bath containing 140 mM NaCl, which was subsequently changed to bath containing 14 mM NaCl osmotically balanced with impermeant mannitol, after which recording was repeated. As noted in the Fig. 3 I–V curves, both APOL1 G0 (Fig. 3A) and G1 (Fig. 3C) exhibited negative shifts in reversal potential (E_{rev}) upon bath transition from 140 mM to 14 mM NaCl. The changes in E_{rev} were −38 mV for APOL1 G0 (Fig. 3A,B p=0.02) and −19 mV for APOL1 G1 (Fig. 3C,D p=0.002). These changes in E_{rev} suggest a cation-to-anion permeability ratio of 4.5 for APOL1 G0-associated currents, and at least 2.1 for APOL1 G1-associated currents, as estimated by the Goldman-Hodgkin-Katz equation. An independent replica set of dilution potential experiments with T-Rex cells induced 18–24 h with doxycycline to express APOL1 G1 revealed E_{rev} shifts consistent with a cation-to-anion permeability ratio of 3.3. These data together document that APOL1-associated whole cell-currents in T-Rex cells exhibit preferential cation selectivity, consistent with previous reports [36,45,30,6].

APOL1-associated whole cell currents are inhibited by rabbit polyclonal antibody raised against APOL1 C-terminal aa 263–387.

The pharmacological signature of APOL1-associated cation currents has been restricted to inhibitors of low affinity and low specificity [21], complicating identification of APOL1-associated currents in the setting of numerous other ion channels expressed in cellular membranes. No small organic molecules, peptides, or antibodies have been reported to inhibit APOL1-associated conductances. As part of a search for APOL1 inhibitors of increased selectivity and potency, we tested commercially available anti-APOL1 antibodies for ability to inhibit APOL1-associated channel activity.

The C-terminal tail of APOL1 is believed to be extracellular, based on reactivity with Serum Response Associated (SRA) [58] and on antibody reactivity [39,20] and topological mutagenesis experiments [40,41]. The I-V curve of Fig. 4A shows that 2–3 min exposure to Sigma rabbit polyclonal IgG raised against human APOL1 C-terminal aa 263–387 IgG (2 μg/ml or ~13 nM) substantially inhibited whole cell currents in HEK-293 T-Rex cells induced to express APOL1 G0, and that inhibition was partially reversible within 3 min after resumption of bath superfusion in the absence of antibody. APOL1 G0-associated

Author Manuscript Author Manuscript Author Manuscript Author Manuscript

currents measured at −100 mV were reduced by 71% in a partially reversible fashion (Fig. 4B), whereas 2 μg/ml non-immune rabbit IgG was without effect (Fig. 4C). Exposure to the same anti-APOL1 antibody (2 μg/ml) similarly inhibited whole cell currents by 58% in HEK-293 T-Rex cells induced to express APOL1 G1 (Fig. 4D, Fig. 4E), whereas the same concentration of non-immune rabbit IgG was again inactive as inhibitor (Fig. 4F).

Interestingly, addition of anti-APOL1 C-terminal domain antibody (2 μg/ml) to 14 mM NaCl bath in the dilution potential experiments of Fig. 2 further left-shifted G0-associated current E_{rev} by −21 mV ($p<0.05$) and further left-shifted G1-associated current E_{rev} by −23 mV ($p<0.05$, data not shown). These data further support the cation channel inhibitory activity of anti-APOL1 C-terminal antibody.

After completion of the experiments in Fig. 4, the work of Scales et al. [39] revealed that the Sigma anti-APOL1 C-terminal region antibody exhibits cross-reactivity with APOL2 by immunofluorescence microscopy and (weakly) by immunoblot in Cos cells overexpressing APOL2. However, the whole cell currents recorded in T-Rex cells doxycycline-induced to overexpress APOL1 likely represent APOL1 activity, as immunoreactive APOL1 was undetected by immunoblot in T-Rex cells expressing empty vector (Fig. 1A).

APOL1-associated whole cell currents are inhibited by rabbit polyclonal antibody raised against APOL1 N-terminal aa 1–238.

Fig. 5A shows an I-V curve from a representative HEK-293 cell induced to express APOL1 G0. Whole cell currents recorded in the absence and in the subsequent presence of Proteintech purified rabbit polyclonal IgG raised against anti-human APOL1 aa 1–238 (2 μg/ml) revealed substantial inhibition of current by the antibody. The summarized data in Fig. 5B for capacitance-normalized APOL1 G0-associated currents measured at −100 mV confirm 45% inhibition by 2–3 min exposure to Proteintech antibody with partial recovery following antibody washout. APOL1 G1-associated whole cell currents were similarly inhibited by Proteintech antibody to the N-terminal region of APOL1 (Fig. 5C). The summarized data for APOL G1-associated whole cell currents measured at −100 mV similarly confirm 53% inhibition in the presence of Proteintech antibody, followed by partial recovery of currents after 3 min antibody washout (Fig. 5D).

After completion of the experiments of Fig. 5, the work of Scales et al [39] revealed that the Proteintech anti-APOL1 N-terminal region antibody exhibits cross-reactivity by immunoblot and by immunofluorescence microscopy with both APOL2 and APOL3 individually overexpressed in Cos cells. However, as noted above, these crossreactivities of the Proteintech antibody do not change the most likely interpretation of the inhibition of doxycycline-induced currents in APOL1-overexpressing T-Rex cells in Fig. 5 as representing inhibition of APOL1-associated currents.

The combined data from HEK-293 T-Rex cells suggest that whole cell currents associated with induced expression of APOL1 G0 or APOL1 G1 can be partially inhibited by antibody raised against most of the C-terminal third of APOL1 G0 or by antibody raised against most of the N-terminal 60% of APOL1 G0, but not by non-specific rabbit IgG. Inhibition by either polyclonal anti-APOL1 antibody was partially reversible upon brief washout.

Author Manuscript Author Manuscript Author Manuscript Author Manuscript

APOL1-associated unitary currents in HEK-293 T-Rex cells.

We applied the on-cell patch clamp configuration to record unitary channel activity associated with induction of APOL1 expression. Fig. 6A shows a representative on-cell current trace of 2.7 s duration of an APOL1 G1-expressing T-Rex cell after 6 h induction with doxycycline. This period of G1 patch clamp activity revealed multiple conductance levels with up to three channels open at any one time, whereas traces recorded from EV-transduced cells showed minimal activity (not shown). All points histogram analysis (ClampFit) of a 30 s period encompassing the APOL1 G1 current trace of Fig. 6A revealed step conductance levels of 2.35 ± 0.27 pA. The Fig. 5B I-V curve reveals a single channel conductance of 27 pS for a representative G1 cell patch with NPo of 1.47. Mean unitary conductance recorded in induced G1 cells was 25.8±1.79 pS (n=7). Fig. 6C summarizes the NPo values measured in on-cell patches of EV cells (0.02±0.003) and G1 cells (1.46±0.22, p=0.006 vs. EV by two-way t-test).

Primary cultured human glomerular podocytes express interferon-γ (IFN γ)-induced currents partially inhibited by anti-APOL1 antibody and abrogated by genetic inactivation of APOL1.

APOL1-associated kidney diseases, including those with the histologic pattern of focal segmental glomerular sclerosis (FSGS), are considered diseases of glomerular podocytes. However APOL1 currents have not previously been characterized in primary cultured human podocytes. Fig. 7A shows that primary cultured human glomerular podocytes (Celprogen) upregulate APOL1 G0 polypeptide following overnight treatment with 10 ng/ml IFNγ. Celprogen primary podocytes maintain a differentiated phenotype, as evidenced by sustained expression of nephrin, podocin and WT1 (Fig. 7B). Overnight exposure to IFNγ (10 ng/ml) also increased by ~4-fold whole cell ramp currents recorded from primary human podocytes (Fig. 7C; Fig. 7E, p=0.016). IFNγ-induced whole cell current was partially inhibited by treatment with 2 μg/ml anti-APOL1 aa 1–238 (Fig. 7D; Fig. 7E, p=0.008), and inhibition was not significantly reversed after 3 min washout (Fig. 7E, right panel). Antibody treatment hyperpolarized whole cell potential by −12.6 ± 2.3 mV (n=7), consistent with inhibition of a current with preferential cation selectivity. The low level of whole cell current in IFNγ-untreated podocytes (Fig.7C) was consistent with low-level expression of APOL1 polypeptide in the absence of IFNγ exposure (Fig. 6A), and was not significantly inhibited by antibody exposure (Fig. 7E, left, p=0.135). We note that IFNγ treatment of immortalized human podocytes has also been reported to increase expression of APOL2 and APOL6 [39], both mediators of channel activity in lipid bilayers [41]. Podocyte immunostaining with a monoclonal antibody to the same N-terminal epitope of APOL1 detected faint, immunospecific plasmalemmaltype staining signal colocalized with Na,K-ATPase in some but not all IFNγ-stimulated Celprogen podocytes (not shown).

On-cell patch recording from Celprogen human primary G0 podocytes treated overnight with 10 ng/ml IFNγ revealed increased single channel activity (Fig. 8A) characterized by a unitary conductance of ~28 pS (Fig. 8B) with near-zero mV reversal potential. The identity of this IFNγ-associated unitary channel of podocytes was tested by comparing clonal, empty vector-transduced Celprogen podocytes with podocyte clones in which APOL1 had been genetically inactivated by the CRISPR-Cas9 method. The immunoblot of Fig. 7A reveals

Author Manuscript Author Manuscript Author Manuscript Author Manuscript

that IFNγ failed to induce accumulation of APOL1 polypeptide in three clonal knockout cell lines. As presented in Fig. 8C, IFNγ exposure increased channel NPo in wild-type podocytes, whereas IFNγ failed to increase current density in two distinct clonal APOL1 knockout cell lines. This result suggests that neither APOL2 nor APOL6, which along with APOL1 are induced by IFNγ treatment of immortalized human podocytes [39] and which both mediate ion channel activity in lipid bilayers [41], contribute significantly to IFNγ-stimulated current measured by on-cell patch recording in Celprogen primary human G0 podocytes. Thus, the IFNγ-stimulated current in Celprogen human podocytes is either APOL1-mediated or requires APOL1 expression for its functional expression in on-cell patch recordings.

IFNγ-stimulated unitary currents of human primary G0 podocytes are blocked by anti-APOL1 antibody and by Serum Resistance-Associated (SRA).

We tested the ability of rabbit polyclonal anti-APOL1 aa 1–238 antibody in the pipette solution to inhibit single channel currents recorded in on-cell patch configuration on Celprogen human primary podocytes expressing APOL1 G0. The anti-APOL1 antibody (2 μg/ml) strongly reduced channel NPo compared to activity recorded in the absence of antibody from the pipette. In contrast, non-specific rabbit IgG added to the pipette solution at the same concentration was not inhibitory (Fig. 9A). We then examined the ability of recombinant SRA N-terminal domain in the pipette solution to inhibit IFNγ-stimulated single channel currents of Celprogen human primary G0 podocytes. Based on the APOL1 binding constant of SRA N-terminal domain of 277 nM as measured by microscale thermophoresis [58], we added a near-saturating concentration of 3 μM SRA to the pipette solution. As shown in Fig. 8B, channel NPo of ~2.2 was recorded in on-cell patch configuration within 10 sec after establishment of a gigohm seal, but channel NPo in the same patches fell to near zero values within <2 min. SRA-sensitivity has not been reported as a property of currents mediated by either APOL2 or APOL6. Moreover, the stable gigaseal on-cell patches achieved in Celprogen podocytes did not correspond to the membrane bilayer instability promoted by recombinant APOL6 [41]. Thus, these data reinforce the identity of the IFNγ-induced unitary cation channels of human primary podocytes as either APOL1-mediated or APOL1-dependent. They further document that SRA applied outside the podocyte can inhibit APOL1-associated single channel currents.

Discussion

The mechanism by which APOL1 risk variants G1 and G2 increase susceptibility to kidney disease remains unclear. Among the numerous proposed mechanisms is that of increased cellular cation permeability conferred by expression of APOL1 G1 and G2 [32]. We have further investigated this property of APOL1, initially in HEK-293 T-Rex cells that inducibly express APOL1. APOL1 undergoes signal sequence cleavage, ER membrane insertion, and post-ER trafficking to multiple subcellular destinations, including plasma membrane. Our studies detected whole cell current density in cells expressing APOL1 G1 and G2 of higher magnitude than those recorded in cells expressing APOL1 G0 (Fig. 1). All three groups of cells exhibited equivalent total abundance of APOL1 protein, with detectable expression at the cell periphery. The currents recorded from HEK-293 T-Rex cells overexpressing APOL1

Author Manuscript Author Manuscript Author Manuscript Author Manuscript

prior to evident cytotoxicity exhibited preferential selectivity for cations over anions (Figs. 2 and 3). These APOL1 currents were inhibited by acid pH, by μM Zn^{2+}, and by mM Gd^{3+} (Fig. 2). Elevated whole cell currents associated with overexpression of APOL1 G0 or G1 were partially inhibited by bath application of either of two commercially available, oligospecific polyclonal antibodies directed against incompletely overlapping portions of the proteins (Figs. 4 and 5). Single channel recording in HEK-293 T-Rex cells induced to overexpress APOL1 G1 revealed a dominant unitary conductance of ~26 pS with NPo of ~1.5.

We have also extended electrophysiological studies to primary human glomerular podocytes expressing endogenous APOL1 G0 (Fig. 7). We documented the presence in these podocytes of IFNγ-inducible whole cell cation currents partially inhibited by bath application of anti-APOL1 antibody (Fig. 7), resembling the currents observed in APOL1-expressing HEK-293 T-Rex cells. The IFNγ-induced unitary currents of primary human podocytes were absent in two oligoclonal podocyte populations (Fig. 8) subjected to CRISPR-Cas9-mediated genetic inactivation of APOL1 (Fig. 7) which abrogated APOL1 polypeptide detection by immunoblot. The unitary currents recorded from IFNγ-stimulated podocytes were nearly completely blocked by addition to the pipette solution of either anti-APOL1 antibody or of SRA (Fig. 9).

We conclude from these experiments that IFNγ-stimulated cation currents in Celprogen (APOL1 G0-expressing) primary cultured human podocytes are most likely mediated by APOL1, or at least require APOL1 expression.

APOL1 mediates or is an essential part of cation channel activity in intact cells

Although recombinant *E. coli*-produced APOL1 has long been recognized as sufficient to promote cation currents in lipid bilayers, its multiple reported cellular localizations and functions, along with its dosedependent cytotoxicity, have raised questions about the role(s) of its channel function in intact mammalian cells. The results of our experiments, most importantly the loss of channel function in APOL1 knockout podocytes, confirm that increased cation currents in cells expressing heterologous or endogenous APOL1 very likely are mediated by plasmalemmal APOL1 itself, consistent with the ability of purified recombinant APOL1 to conduct cations in planar lipid bilayers [45] and in reconstituted proteoliposomes [7]. Although APOL1 polypeptide suffices to mediate channel activity in bilayers and proteoliposomes, we cannot state definitively that APOL1 acts alone to generate this ion conductance in cultured cells or *in vivo*. Although APOL1 expression is necessary for cellular channel activity that can be blocked by oligospecific antibodies and by *T. brucei* SRA, the possibility remains that APOL1 in mammalian cells constitutes a subunit within a cellular multi-protein complex that includes one or more additional channels, channel modulators or gating factors. Whether APOL1 acts alone or in complex as a cation channel, the possible contribution of APOL1 channel activity to ER stress [25], altered lipid droplet metabolism [10,9], mitochondrial dysfunction [42], cytoskeletal alteration by phosphatidyl-inositol phosphate dysregulation [48], PKR activation [31], and NLRP3/STING pathway activation [54] remains uncertain in kidney as well as in extrarenal tissues [53].

Author Manuscript Author Manuscript Author Manuscript Author Manuscript

Anti-APOL1 antibodies partially inhibit APOL1-mediated channel activity.

The antibodies used to inhibit APOL1 activity were later shown to be cross-reactive with overexpressed APOL2 or with APOL2 and APOL3 by immunoblot and/or immunocytochemistry [39]. We found that these antibodies inhibited current that was induced by doxycycline-induced overexpression of heterologous APOL1. Moreover, IFNγ-induced currents of Celprogen human primary podocytes that were partially inhibited by anti-APOL1 antibody were abrogated in Celprogen podocytes subjected to CRISPR-Cas9 knockout of APOL1 using two different APOL1-specific guide RNAs. Currents potentially attributable to INFγ-induced APOL2 or APOL6 [39,41] were not apparent in the setting of APOL1 knockout. Thus, despite the lack of complete APOL1-specificity of the commercial antibodies tested in this work, their ability to partially inhibit cation currents in doxycycline-induced HEK-293 T-Rex cells as well as in IFNγ-stimulated Celprogen human primary podocytes very likely represents inhibition of APOL1-associated channel activity (or APOL1-dependent activity of another cation channel).

Functionally inhibitory antibodies to ion channels and solute transporters have traditionally been difficult to generate [22], but new strategies are expanding the repertoire of transport-inhibitory antibodies [55]. The structure of the APOL1 transmembrane domain remains unknown, with antibody accessibility studies and electrophysiological analysis of mutant polypeptides yielding different topographical models of APOL1's disposition within the plasma membrane [20,40]. APOL1 antibodies might inhibit APOL1-mediated channel activity by direct pore block or by binding to a "distant site" with a negative allosteric impact on the channel pore. Camelid "synbodies" [12] might be of optimal use in distinguishing between these possibilities.

The polyclonal antibodies tested in this study to inhibited a fraction of APOL1-associated whole cell current in HEK-293 T-Rex cells that appeared rapidly reversible upon antibody washout. Rapid reversibility of antibody-mediated inhibition has been previously, if infrequently, reported in studies of functional antibodies directed against the M3 muscarinic receptor [11] and against the TRPV2 cation channel [24]. The component of anti-APOL1 antibody-mediated inhibition of current that appeared reversible may reflect a subset of immunoglobulins within the polyclonal antibody mixture with accelerated off-rates (perhaps including components cross-reactive with APOL2 and/or APOL3).

The poorly reversible component of anti-APOL1 antibody-mediated channel inhibition might represent promotion by antibody binding of APOL1 endocytosis from the plasma membrane. Preliminary experiments with the modestly specific endocytosis inhibitors Dyngo-4 and Pitstop [23] have suggested support for this hypothesis, which can be more specifically addressed by direct monitoring of surface-biotinylatable APOL1 and through genetic inactivation of individual endocytic pathways. Tests of additional ecto-reactive anti-APOL1 antibodies [39] for anti-channel activity in HEK-293 T-Rex cells and in podocytes will also be of great interest.

Anti-APOL1 antibody-mediated inhibition of IFNγ-stimulated APOL1-associated current in Celprogen podocytes (Fig. 7) was less reversible than APOL1-associated current in HEK-293 T-Rex cells (Figs. 4 and 5). This difference might relate to increased podocyte

Author Manuscript Author Manuscript Author Manuscript Author Manuscript

expression of Fc receptors. Primary mouse express levels of the Fc receptors FcRgIIB and FcRgIII which decrease over time in cell culture, whereas dimeric Fc receptor FcRn levels are high upon plating and remain elevated [2]. Anti-APOL1 antibody bound to APOL1 on the podocyte surface might thus more likely be clustered and endocytosed than in HEK-293 T-Rex cells. Such endocytosis might contribute to the near-complete inhibition of on-cell patch current by antibody applied to the cell surface in the patch pipette solution (Fig. 9).

What is the role of APOL1-associated cation channel activity in cytotoxicity?

Increased APOL1 expression-mediated depletion of intracellular [K^+] [33] and elevation of intracellular [Ca^{2+}] and intracellular [Na^+] have been associated with later cytotoxicity in HEK-293 cells and in HeLa cells [18]. This later cytotoxicity has been associated with still greater and more abrupt elevations in intracellular [Ca^{2+}] in parallel with APOL1 delivery from ER to the cell surface, followed by later cell rupture and death [18]. APOL1 trafficking to the cell surface and cell death was detectable in only a small proportion of cells overexpressing APOL1 on the time scale of these experiments, and trafficking of APOL1 G1 appeared more efficient than that of APOL1 G2.

If APOL1 channel activity is the primary cause of cytotoxicity, then the channel activities of risk variants G1 and G2 should exceed that of G0. Our results show that HEK-293 T-Rex cells induced to express APOL1 G1 exhibit whole cell currents of magnitude higher than recorded in cells expressing APOL1 G0 at comparable total abundance. These results contrast with a previous report in which risk variant-associated whole cell currents were equivalent in magnitude to G0-associated currents [30]. The difference in outcomes may reflect the recently reported differences in APOL1 incorporation into proteoliposomes not only as a function of risk variant [6], but also as a function of risk variant- and ethnicity-associated haplotype [26,52], possibly reflected in the undescribed APOL1 variant sequences used in the earlier study [30]. Thus, increased current magnitude may account for risk variant-specific APOL1 cytotoxicity (at least in induced HEK-293 T-Rex cells), perhaps reflecting increased APOL1 riskvariant affinity for lipid membranes [6,52], itself possibly contributing to increased APOL1 cell surface expression [6].

If cation channel activity is the primary contributor to APOL1 risk variant cytotoxicity, then inhibition of channel activity should prevent cytotoxicity. Indeed, Cys-substitution mutant polypeptides that exhibit loss of channel function in lipid bilayer reconstitution experiments also exhibit loss of trypanolytic efficacy [41]. Tests of the ability of anti-APOL1 antibodies to attenuate APOL1-associated cytotoxicity are ongoing, and will benefit from use of antibodies of higher specificity [39].

Tests of whether inhibition of APOL1 channel activity suffices to prevent cytotoxicity will best exploit engineered mutations that reduce or abolish channel activity without reducing apparent polypeptide expression or membrane incorporation [40,41]. Schaub et al. have proposed that channel activation requires APOL1 oligomerization via intermolecular coiled-coil formation [40] which, in turn, requires destabilization of the native intramolecular hairpin consisting of the TM4 pore-lining residues and the C-terminal coiled-coil domain of monomeric APOL1 [43]. The lower apparent stability of the monomeric intramolecular coiled-coil of APOL1 renal risk variants G1 and G2 than that of G0 [43] could explain

Author Manuscript Author Manuscript Author Manuscript Author Manuscript

at least part of the increased cytotoxicity of risk variant polypeptides relative to G0. Indeed, multiple simultaneous Leu-to-Ala substitutions that disrupt intermolecular coiled-coil formation and oligomerization were reported to reduce APOL1 G0 cytotoxicity in cultured cells [40]. Ultimately, the role of APOL1 channel activity in disease severity will be most directly tested by generation of transgenic mice expressing APOL1 renal risk variants carrying channel-inactivating mutations in the pore-lining [41] or C-terminal coiled-coil helices [40], and assessing their susceptibility to IFNγ-induced proteinuria and CKD [27,3] or to APOL1-associated extrarenal pathology [53].

Are Celprogen primary human podocytes in culture good models of glomerular podocytes for the study of APOL1?

Ts-SV40 LgT-immortalized human and mouse podocytes have been instrumental in advancing our understanding of podocyte biology, despite problems with *in vitro* maintenance of differentiation state [19,38]. Podocyte lines immortalized from human urine can respond to poly-I:C with induction of detectable APOL1 expression. However, cytotoxicity measured as cell viability, podocyte detachment and elevated apoptosis was noted to be variant-independent in these cell lines [14].

The Celprogen primary human podocytes used in our studies retain a differentiated phenotype, with expression of nephrin, podocin and WT1 (Fig. 7) resembling that documented in human kidney organoids [9]. Our recordings from primary human podocytes were complemented by preliminary studies in which primary murine podocytes were outgrown overnight on rat tail collagen after isolation from IFNγ-treated and -untreated APOL1 G2 knock-in mice [27]. On-cell patch recording revealed G2 knock-in mouse podocyte cation currents with unitary conductance of 25.2±2.5 pS and NPo of 1.41±0.24 (n=3, −Vp = +50 mV, data not shown), similar to values recorded in on-cell patches of IFNγ-treated Celprogen human G0 podocytes (Fig. 8).

Future recording from intact podocytes of glomeruli isolated from BAC-transgenic APOL1 mice treated without or with IFNγ will allow correlation of channel activity with proteinuria and glomerular histopathological changes. Parallel track experiments will be conducted with glomeruli in kidney organoids differentiated from induced pluripotent stem cells expressing APOL1 G0, G1 or G2 [9,51].

Limitations and conclusions:

Our data are limited by their reliance on oligospecific polyclonal antibodies and immortalized and primary cells passaged in tissue culture. In particular, our experiments utilizing HEK-293 T-Rex cells are subject to distortion by possible off-target effects of the inducer doxycycline, known, for example, to inhibit mitochondrial protein synthesis at higher concentrations than used here. These data are also subject to distortion by “subclinical cytotoxicity” of APOL1, which we attempted to minimize by measuring experimental outcomes after 6 h induction (or 10 h for immunolocalization). Many of the characteristics of APOL1-associated currents detected in HEK-293 T-Rex cells were reproduced in primary human podocytes in culture. However, as Celprogen podocytes express APOL1 G0, future experiments will compare currents of APOL1 risk variants G1

and G2 with G0 in human induced pluripotent stem cell-derived podocytes, in transgenic mouse podocytes in the contexts of isolated intact glomeruli and of primary glomerular outgrowths, and in BAC-transgenic mice expressing APOL1 G0, G1, or G2 in uniform insertion sites [27], bred to express podocyte-specific genetically endcoded Ca^{2+} indicators.

In summary, we have shown that HEK-293 cells overexpressing APOL1 risk variants expressed currents of higher magnitude than did cells overexpressing APOL1 G0. These currents displayed preferential cation selectivity and were partially inhibited by extracellular exposure to oligospecific anti-APOL1 antibodies. Similar currents were induced by IFNγ in Celprogen primary human podocytes of APOL1 G0 genotype. These currents were inhibited by extracellular anti-APOL1 antibody and by extracellular trypanosomal protein SRA, and were abrogated by CRISPR-mediated knockout of the *APOL1* gene. We conclude that APOL1 mediates IFNγ-induced cation currents in human primary glomerular podocytes, or is at least required for expression of those currents.

Acknowledgements:

We acknowledge helpful discussions with Dr. Justin Chun (now at the University of Calgary, Calgary, Alberta), Dr. Jiayue Zhang (now at Frontera Therapeutics, Winchester, MA), Dr. Alok K. Sharma (now at Frederick National Laboratory for Cancer Research and Leidos Biomedical Research, Frederick MD), and Dr. Johannes Schlondorff of Beth Israel Deaconess Medical Center and Harvard Medical School (now at the Ohio State University School of Medicine).

Funding:

This work was supported by research grants from NIMHD to MRP, SLA, and DJF, and by a grant to MRP from the Ellison Foundation.

Availability of supporting data:

Supporting data are available upon request.

References

1. Aghajan M, Booten SL, Althage M, Hart CE, Ericsson A, Maxvall I, Ochaba J, Menschik-Lundin A, Hartleib J, Kuntz S, Gattis D, Ahlstrom C, Watt AT, Engelhardt JA, Monia BP, Magnone MC, Guo S (2019) Antisense oligonucleotide treatment ameliorates IFN-gamma-induced proteinuria in APOL1-transgenic mice. JCI Insight 4. doi:10.1172/jci.insight.126124
2. Akilesh S, Huber TB, Wu H, Wang G, Hartleben B, Kopp JB, Miner JH, Roopenian DC, Unanue ER, Shaw AS (2008) Podocytes use FcRn to clear IgG from the glomerular basement membrane. Proc Natl Acad Sci U S A 105:967–972. doi:10.1073/pnas.0711515105 [PubMed: 18198272]
3. Beckerman P, Bi-Karchin J, Park AS, Qiu C, Dummer PD, Soomro I, Boustany-Kari CM, Pullen SS, Miner JH, Hu CA, Rohacs T, Inoue K, Ishibe S, Saleem MA, Palmer MB, Cuervo AM, Kopp JB, Susztak K (2017) Transgenic expression of human APOL1 risk variants in podocytes induces kidney disease in mice. Nat Med 23:429–438. doi:10.1038/nm.4287 [PubMed: 28218918]
4. Bruggeman LA, Sedor JR, O'Toole JF (2021) Apolipoprotein L1 and mechanisms of kidney disease susceptibility. Curr Opin Nephrol Hypertens 30:317–323. doi:10.1097/MNH.0000000000000704 [PubMed: 33767059]
5. Bruggeman LA, Wu Z, Luo L, Madhavan SM, Konieczkowski M, Drawz PE, Thomas DB, Barisoni L, Sedor JR, O'Toole JF (2016) APOL1-G0 or APOL1-G2 Transgenic Models Develop Preeclampsia but Not Kidney Disease. J Am Soc Nephrol 27:3600–3610. doi:10.1681/ASN.2015111220 [PubMed: 27026370]

Author Manuscript Author Manuscript Author Manuscript Author Manuscript

Author Manuscript Author Manuscript Author Manuscript Author Manuscript

6. Bruno J, Edwards JC (2021) Kidney-disease-associated variants of Apolipoprotein L1 show gain of function in cation channel activity. J Biol Chem 296:100238. doi:10.1074/jbc.RA120.013943
7. Bruno J, Pozzi N, Oliva J, Edwards JC (2017) Apolipoprotein L1 confers pH-switchable ion permeability to phospholipid vesicles. J Biol Chem 292:18344–18353. doi:10.1074/jbc.M117.813444 [PubMed: 28918394]
8. Campillo N, Carrington M (2003) The origin of the serum resistance associated (SRA) gene and a model of the structure of the SRA polypeptide from Trypanosoma brucei rhodesiense. Mol Biochem Parasitol 127:79–84. doi:10.1016/s0166-6851(02)00306-7 [PubMed: 12615339]
9. Chun J, Riella C, Hyunjae C, Shah S, Wang M, Magraner J, Ribas G, Ribas H, Zhang JY, Alper S, Friedman D and Pollak M (2022) DGAT2 Inhibition Potentiates Lipid Droplet Formation to Reduce Cytotoxicity in APOL1 Kidney Risk Variants. JASN:in press. doi:10.1681/ASN.2021050723
10. Chun J, Zhang JY, Wilkins MS, Subramanian B, Riella C, Magraner JM, Alper SL, Friedman DJ, Pollak MR (2019) Recruitment of APOL1 kidney disease risk variants to lipid droplets attenuates cell toxicity. Proc Natl Acad Sci U S A 116:3712–3721. doi:10.1073/pnas.1820414116 [PubMed: 30733285]
11. Dawson LJ, Stanbury J, Venn N, Hasdimir B, Rogers SN, Smith PM (2006) Antimuscarinic antibodies in primary Sjogren's syndrome reversibly inhibit the mechanism of fluid secretion by human submandibular salivary acinar cells. Arthritis Rheum 54:1165–1173. doi:10.1002/art.21764 [PubMed: 16572451]
12. Deneka D, Rutz S, Hutter CAJ, Seeger MA, Sawicka M, Dutzler R (2021) Allosteric modulation of LRRC8 channels by targeting their cytoplasmic domains. Nat Commun 12:5435. doi:10.1038/s41467-021-25742-w [PubMed: 34521847]
13. Doench JG, Fusi N, Sullender M, Hegde M, Vaimberg EW, Donovan KF, Smith I, Tothova Z, Wilen C, Orchard R, Virgin HW, Listgarten J, Root DE (2016) Optimized sgRNA design to maximize activity and minimize off-target effects of CRISPR-Cas9. Nat Biotechnol 34:184–191. doi:10.1038/nbt.3437 [PubMed: 26780180]
14. Ekulu PM, Adebayo OC, Decuypere JP, Bellucci L, Elmonem MA, Nkoy AB, Mekahli D, Bussolati B, van den Heuvel LP, Arcolino FO, Levtchenko EN (2021) Novel Human Podocyte Cell Model Carrying G2/G2 APOL1 High-Risk Genotype. Cells 10. doi:10.3390/cells10081914
15. Friedman DJ, Pollak MR (2020) APOL1 and Kidney Disease: From Genetics to Biology. Annu Rev Physiol 82:323–342. doi:10.1146/annurev-physiol-021119-034345 [PubMed: 31710572]
16. Friedman DJ, Pollak MR (2021) APOL1 Nephropathy: From Genetics to Clinical Applications. Clin J Am Soc Nephrol 16:294–303. doi:10.2215/CJN.15161219 [PubMed: 32616495]
17. Genovese G, Friedman DJ, Ross MD, Lecordier L, Uzureau P, Freedman BI, Bowden DW, Langefeld CD, Oleksyk TK, Uscinski Knob AL, Bernhardy AJ, Hicks PJ, Nelson GW, Vanhollebeke B, Winkler CA, Kopp JB, Pays E, Pollak MR (2010) Association of trypanolytic ApoL1 variants with kidney disease in African Americans. Science 329:841845. doi:10.1126/science.1193032
18. Giovinazzo JA, Thomson RP, Khalizova N, Zager PJ, Malani N, Rodriguez-Boulan E, Raper J, Schreiner R (2020) Apolipoprotein L-1 renal risk variants form active channels at the plasma membrane driving cytotoxicity. Elife 9. doi:10.7554/eLife.51185
19. Greka A, Mundel P (2012) Cell biology and pathology of podocytes. Annu Rev Physiol 74:299–323. doi:10.1146/annurev-physiol-020911-153238 [PubMed: 22054238]
20. Gupta N, Wang X, Wen X, Moran P, Paluch M, Hass PE, Heidersbach A, Haley B, Kirchhofer D, Brezski RJ, Peterson AS, Scales SJ (2020) Domain-Specific Antibodies Reveal Differences in the Membrane Topologies of Apolipoprotein L1 in Serum and Podocytes. J Am Soc Nephrol 31:2065–2082. doi:10.1681/ASN.2019080830 [PubMed: 32764138]
21. Heneghan JF, Vandorpe DH, Shmukler BE, Giovinazzo JA, Raper J, Friedman DJ, Pollak MR, Alper SL (2015) BH3 domain-independent apolipoprotein L1 toxicity rescued by BCL2 prosurvival proteins. Am J Physiol Cell Physiol 309:C332–347. doi:10.1152/ajpcell.00142.2015 [PubMed: 26108665]
22. Hutchings CJ, Colussi P, Clark TG (2019) Ion channels as therapeutic antibody targets. MAbs 11:265–296. doi:10.1080/19420862.2018.1548232 [PubMed: 30526315]

Author Manuscript Author Manuscript Author Manuscript Author Manuscript

23. Ivanov AI (2014) Pharmacological inhibitors of exocytosis and endocytosis: novel bullets for old targets. Methods Mol Biol 1174:3–18. doi:10.1007/978-1-4939-0944-5_1

24. Iwata Y, Wakabayashi S, Ito S, Kitakaze M (2020) Production of TRPV2-targeting functional antibody ameliorating dilated cardiomyopathy and muscular dystrophy in animal models. Lab Invest 100:324–337. doi:10.1038/s41374-019-0363-1 [PubMed: 31896817]

25. Kumar V, Singhal PC (2019) APOL1 and kidney cell function. Am J Physiol Renal Physiol 317:F463–F477. doi:10.1152/ajprenal.00233.2019 [PubMed: 31241995]

26. Lannon H, Shah SS, Dias L, Blackler D, Alper SL, Pollak MR, Friedman DJ (2019) Apolipoprotein L1 (APOL1) risk variant toxicity depends on the haplotype background. Kidney Int 96:1303–1307. doi:10.1016/j.kint.2019.07.010 [PubMed: 31611067]

27. McCarthy GM, Blasio A, Donovan OG, Schaller LB, Bock-Hughes A, Magraner JM, Suh JH, Tattersfield CF, Stillman IE, Shah SS, Zsengeller ZK, Subramanian B, Friedman DJ, Pollak MR (2021) Recessive, gain-of-function toxicity in an APOL1 BAC transgenic mouse model mirrors human APOL1 kidney disease. Dis Model Mech 14. doi:10.1242/dmm.048952

28. Molina-Portela Mdel P, Lugli EB, Recio-Pinto E, Raper J (2005) Trypanosome lytic factor, a subclass of high-density lipoprotein, forms cation-selective pores in membranes. Mol Biochem Parasitol 144:218–226. doi:10.1016/j.molbiopara.2005.08.018 [PubMed: 16202458]

29. Nichols B, Jog P, Lee JH, Blackler D, Wilmot M, D'Agati V, Markowitz G, Kopp JB, Alper SL, Pollak MR, Friedman DJ (2015) Innate immunity pathways regulate the nephropathy gene Apolipoprotein L1. Kidney Int 87:332–342. doi:10.1038/ki.2014.270 [PubMed: 25100047]

30. O'Toole JF, Schilling W, Kunze D, Madhavan SM, Konieczkowski M, Gu Y, Luo L, Wu Z, Bruggeman LA, Sedor JR (2018) ApoL1 Overexpression Drives Variant-Independent Cytotoxicity. J Am Soc Nephrol 29:869–879. doi:10.1681/ASN.2016121322 [PubMed: 29180397]

31. Okamoto K, Rausch JW, Wakashin H, Fu Y, Chung JY, Dummer PD, Shin MK, Chandra P, Suzuki K, Shrivastav S, Rosenberg AZ, Hewitt SM, Ray PE, Noiri E, Le Grice SFJ, Hoek M, Han Z, Winkler CA, Kopp JB (2018) APOL1 risk allele RNA contributes to renal toxicity by activating protein kinase R. Commun Biol 1:188. doi:10.1038/s42003-018-0188-2 [PubMed: 30417125]

32. Olabisi OA, Heneghan JF (2017) APOL1 Nephrotoxicity: What Does Ion Transport Have to Do With It? Semin Nephrol 37:546–551. doi:10.1016/j.semnephrol.2017.07.008 [PubMed: 29110762]

33. Olabisi OA, Zhang JY, VerPlank L, Zahler N, DiBartolo S 3rd, Heneghan JF, Schlondorff JS, Suh JH, Yan P, Alper SL, Friedman DJ, Pollak MR (2016) APOL1 kidney disease risk variants cause cytotoxicity by depleting cellular potassium and inducing stress-activated protein kinases. Proc Natl Acad Sci U S A 113:830–837. doi:10.1073/pnas.1522913113 [PubMed: 26699492]

34. Papeta N, Kiryluk K, Patel A, Sterken R, Kacak N, Snyder HJ, Imus PH, Mhatre AN, Lawani AK, Julian BA, Wyatt RJ, Novak J, Wyatt CM, Ross MJ, Winston JA, Klotman ME, Cohen DJ, Appel GB, D'Agati VD, Klotman PE, Gharavi AG (2011) APOL1 variants increase risk for FSGS and HIVAN but not IgA nephropathy. J Am Soc Nephrol 22:1991–1996. doi:10.1681/ASN.2011040434 [PubMed: 21997397]

35. Pays E, Vanhollebeke B, Uzureau P, Lecordier L, Perez-Morga D (2014) The molecular arms race between African trypanosomes and humans. Nat Rev Microbiol 12:575–584. doi:10.1038/nrmicro3298 [PubMed: 24975321]

36. Perez-Morga D, Vanhollebeke B, Paturiaux-Hanocq F, Nolan DP, Lins L, Homble F, Vanhamme L, Tebabi P, Pays A, Poelvoorde P, Jacquet A, Brasseur R, Pays E (2005) Apolipoprotein L-I promotes trypanosome lysis by forming pores in lysosomal membranes. Science 309:469–472. doi:10.1126/science.1114566 [PubMed: 16020735]

37. Qian T, Hernday SE, Bao X, Olson WR, Panzer SE, Shusta EV, Palecek SP (2019) Directed Differentiation of Human Pluripotent Stem Cells to Podocytes under Defined Conditions. Sci Rep 9:2765. doi:10.1038/s41598-019-39504-8 [PubMed: 30808965]

38. Saleem MA (2015) One hundred ways to kill a podocyte. Nephrol Dial Transplant 30:12661271. doi:10.1093/ndt/gfu363

39. Scales SJ, Gupta N, De Maziere AM, Posthuma G, Chiu CP, Pierce AA, Hotzel K, Tao J, Foreman O, Koukos G, Oltrabella F, Klumperman J, Lin W, Peterson AS (2020) Apolipoprotein L1-Specific Antibodies Detect Endogenous APOL1 inside the Endoplasmic Reticulum and on the Plasma

Author Manuscript Author Manuscript Author Manuscript Author Manuscript

Membrane of Podocytes. J Am Soc Nephrol 31:2044–2064. doi:10.1681/ASN.2019080829 [PubMed: 32764142]

40. Schaub C, Lee P, Racho-Jansen A, Giovinazzo J, Terra N, Raper J, Thomson R (2021) Coiledcoil binding of the leucine zipper domains of APOL1 is necessary for the open cation channel conformation. J Biol Chem 297:101009. doi:10.1016/j.jbc.2021.101009
41. Schaub C, Verdi J, Lee P, Terra N, Limon G, Raper J, Thomson R (2020) Cation channel conductance and pH gating of the innate immunity factor APOL1 are governed by pore-lining residues within the C-terminal domain. J Biol Chem 295:13138–13149. doi:10.1074/jbc.RA120.014201 [PubMed: 32727852]
42. Shah SS, Lannon H, Dias L, Zhang JY, Alper SL, Pollak MR, Friedman DJ (2019) APOL1 Kidney Risk Variants Induce Cell Death via Mitochondrial Translocation and Opening of the Mitochondrial Permeability Transition Pore. J Am Soc Nephrol 30:2355–2368. doi:10.1681/ASN.2019020114 [PubMed: 31558683]
43. Sharma AK, Friedman DJ, Pollak MR, Alper SL (2016) Structural characterization of the C-terminal coiled-coil domains of wild-type and kidney disease-associated mutants of apolipoprotein L1. FEBS J 283:1846–1862. doi:10.1111/febs.13706 [PubMed: 26945671]
44. Talbot BE, Vandorpe DH, Stotter BR, Alper SL, Schlondorff JS (2019) Transmembrane insertases and N-glycosylation critically determine synthesis, trafficking, and activity of the nonselective cation channel TRPC6. J Biol Chem 294:12655–12669. doi:10.1074/jbc.RA119.008299 [PubMed: 31266804]
45. Thomson R, Finkelstein A (2015) Human trypanolytic factor APOL1 forms pH-gated cation-selective channels in planar lipid bilayers: relevance to trypanosome lysis. Proc Natl Acad Sci U S A 112:2894–2899. doi:10.1073/pnas.1421953112 [PubMed: 25730870]
46. Thomson R, Genovese G, Canon C, Kovacsics D, Higgins MK, Carrington M, Winkler CA, Kopp J, Rotimi C, Adeyemo A, Doumatey A, Ayodo G, Alper SL, Pollak MR, Friedman DJ, Raper J (2014) Evolution of the primate trypanolytic factor APOL1. Proc Natl Acad Sci U S A 111:E2130–2139. doi:10.1073/pnas.1400699111 [PubMed: 24808134]
47. Tzur S, Rosset S, Shemer R, Yudkovsky G, Selig S, Tarekegn A, Bekele E, Bradman N, Wasser WG, Behar DM, Skorecki K (2010) Missense mutations in the APOL1 gene are highly associated with end stage kidney disease risk previously attributed to the MYH9 gene. Hum Genet 128:345–350. doi:10.1007/s00439-010-0861-0 [PubMed: 20635188]
48. Uzureau S, Lecordier L, Uzureau P, Hennig D, Graversen JH, Homble F, Mfutu PE, Oliveira Arcolino F, Ramos AR, La Rovere RM, Luyten T, Vermeersch M, Tebabi P, Dieu M, Cuypers B, Deborggraeve S, Rabant M, Legendre C, Moestrup SK, Levtchenko E, Bultynck G, Erneux C, Perez-Morga D, Pays E (2020) APOL1 C-Terminal Variants May Trigger Kidney Disease through Interference with APOL3 Control of Actomyosin. Cell Rep 30:3821–3836 e3813. doi:10.1016/j.celrep.2020.02.064 [PubMed: 32187552]
49. Vanwalleghem G, Fontaine F, Lecordier L, Tebabi P, Klewe K, Nolan DP, Yamaryo-Botte Y, Botte C, Kremer A, Burkard GS, Rassow J, Roditi I, Perez-Morga D, Pays E (2015) Coupling of lysosomal and mitochondrial membrane permeabilization in trypanolysis by APOL1. Nat Commun 6:8078. doi:10.1038/ncomms9078 [PubMed: 26307671]
50. Waters JP, Richards YC, Skepper JN, Southwood M, Upton PD, Morrell NW, Pober JS, Bradley JR (2017) A 3D tri-culture system reveals that activin receptor-like kinase 5 and connective tissue growth factor drive human glomerulosclerosis. J Pathol 243:390–400. doi:10.1002/path.4960 [PubMed: 28815607]
51. Williams S, Charest JL, Pollak MR, Subramanian B (2022) Bioengineering Strategies to Develop Podocyte Culture Systems. Tissue Eng Part B Rev 28:938–948. doi:10.1089/ten.TEB.2021.0154 [PubMed: 34541902]
52. Winkler RL, Bruno J, Buchanan P, Edwards JC (2022) Cation Channel Activity of Apolipoprotein L1 is Modulated by Haplotype Background. J Am Soc Nephrol. doi:10.1681/ASN.2022020213
53. Wu J, Ma Z, Raman A, Beckerman P, Dhillon P, Mukhi D, Palmer M, Chen HC, Cohen CR, Dunn T, Reilly J, Meyer N, Shashaty M, Arany Z, Hasko G, Laudanski K, Hung A, Susztak K (2021) APOL1 risk variants in individuals of African genetic ancestry drive endothelial cell defects that exacerbate sepsis. Immunity 54:2632–2649 e2636. doi:10.1016/j.immuni.2021.10.004 [PubMed: 34715018]

Author Manuscript Author Manuscript Author Manuscript Author Manuscript

54. Wu J, Raman A, Coffey NJ, Sheng X, Wahba J, Seasock MJ, Ma Z, Beckerman P, Laczko D, Palmer MB, Kopp JB, Kuo JJ, Pullen SS, Boustany-Kari CM, Linkermann A, Susztak K (2021) The key role of NLRP3 and STING in APOL1-associated podocytopathy. J Clin Invest 131. doi:10.1172/JCI136329

55. Wulff H, Christophersen P, Colussi P, Chandy KG, Yarov-Yarovoy V (2019) Antibodies and venom peptides: new modalities for ion channels. Nat Rev Drug Discov 18:339–357. doi:10.1038/s41573-019-0013-8 [PubMed: 30728472]

56. Zahr RS, Rampersaud E, Kang G, Weiss MJ, Wu G, Davis RL, Hankins JS, Estepp JH, Lebensburger J (2019) Children with sickle cell anemia and APOL1 genetic variants develop albuminuria early in life. Haematologica 104:e385–e387. doi:10.3324/haematol.2018.212779 [PubMed: 30890594]

57. Zhang JY, Wang M, Tian L, Genovese G, Yan P, Wilson JG, Thadhani R, Mottl AK, Appel GB, Bick AG, Sampson MG, Alper SL, Friedman DJ, Pollak MR (2018) UBD modifies APOL1-induced kidney disease risk. Proc Natl Acad Sci U S A 115:3446–3451. doi:10.1073/pnas.1716113115 [PubMed: 29531077]

58. Zoll S, Lane-Serff H, Mehmood S, Schneider J, Robinson CV, Carrington M, Higgins MK (2018) The structure of serum resistance-associated protein and its implications for human African trypanosomiasis. Nat Microbiol 3:295–301. doi:10.1038/s41564-017-0085-3 [PubMed: 29358741]

Author Manuscript Author Manuscript Author Manuscript Author Manuscript

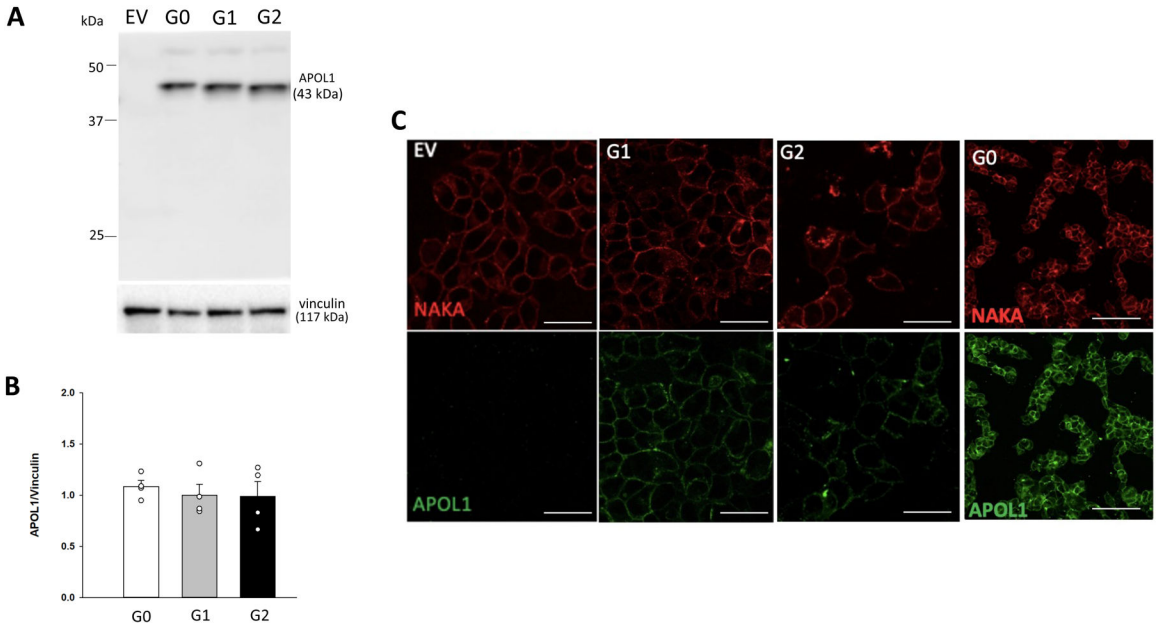

Figure 1. APOL1 expression in HEK-293 T-Rex cells.

A. Representative immunoblot of 6 h doxycycline-induced APOL1 expression in cells stably transfected with empty vector (EV) or vectors encoding APOL1 variants with Lys (G0) or Glu (G1 and G2) at residue 150. Anti-APOL1 antibody was Sigma HPA018885. Vinculin served as loading control. **B.** Densitometric quantitation of APOL1 immunoblots (n=4) similar to that in panel A. Similar results were obtained using GAPDH or β-actin as controls (not shown). **C.** Immunofluorescence micrographs of T-Rex cells stably transfected with EV, G1, G2 (scale bars, 30 μm) or G0 (scale bars, 100 μm), grown on coverslips and treated with doxycycline for 10 h to induce APOL1 expression. Fixed cells were not detergent-permeabilized before antibody incubations. Red represents Na^+,K^+-ATPase α subunit (NAKA); green depicts APOL1. Anti-APOL1 antibody was Proteintech 11486–2-AP.

Author Manuscript
Author Manuscript
Author Manuscript
Author Manuscript

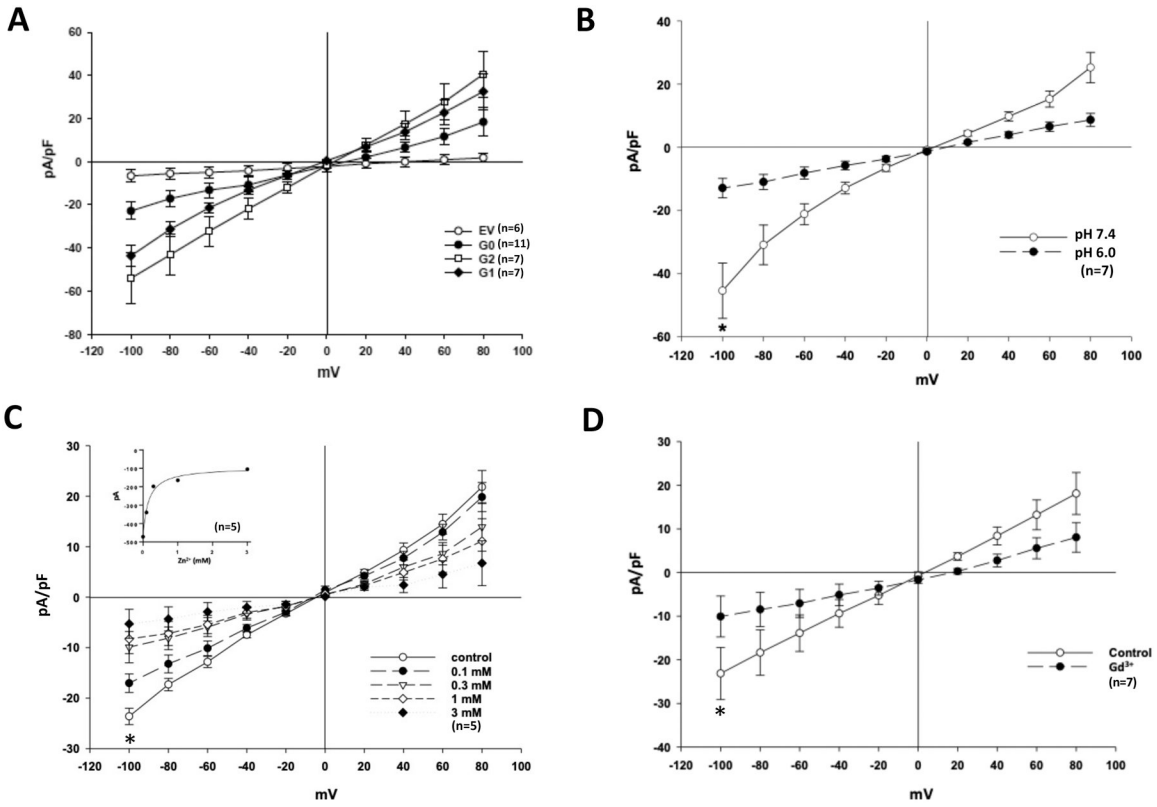

Figure 2. Overexpression of APOL1 G0 and of APOL1 G1 in T-Rex cells leads to increased whole cell currents sensitive to inhibition by acid pH, Zn^{2+}, and Gd^{3+}.

A. Whole cell current-voltage (I-V) curves of T-Rex cells induced 6 h to express EV (open circles, n=6), APOL1 G0 (filled circles, n=11), G1 (filled diamonds, n=7), and G2 (open squares, n=7). Comparison of capacitance-normalized current values at −100 mV revealed p=0.052 for EV vs. G0, p=0.002 for EV vs. G1, p=<0.001 for EV vs G2, p=0.023 for G0 vs G1 and p=0.003 for G0 vs G2 by one-way ANOVA with Bonferroni post-test; two-tailed t-test revealed p=0.0061 for EV vs G0. **B.** Acidic bath pH 6 suppressed whole cell currents in T-Rex cells induced to express APOL1 G1 (n=7; *, p=0.012 by paired two-tailed t-test). **C.** Whole cell I-V curves from T-Rex cells induced to express APOL1 G1, recorded in the presence of sequentially increasing bath concentrations of $ZnSO_4$ (n=5; p=0.001 for 3 mM vs. control at −100 mV; paired two-tailed t-test). Inset: hyperbolic fit of concentration-response curve, showing $ZnSO_4$ IC_{50} of 154 μM. **D.** Whole cell I-V curves from T-Rex cells induced to express APOL1 G1, recorded in the absence (control) and subsequent presence of 1 mM bath $GdCl_3$ (n=7, *, p=0.007 at −100 mV; paired two-tailed t-test).

Author Manuscript Author Manuscript Author Manuscript Author Manuscript

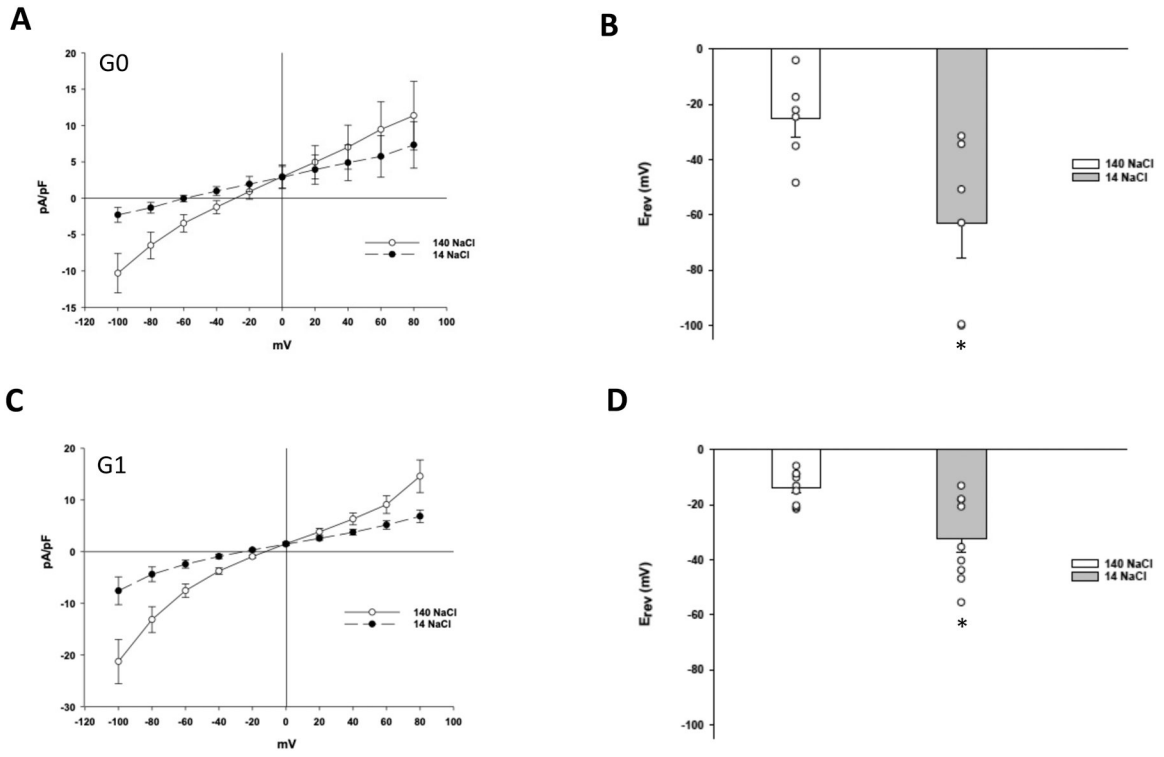

Figure 3. APOL1-associated channel activity exhibits preferential cation selectivity.

A. Representative whole cell I-V curve of T-Rex cells induced 6 h to express APOL1 G0, recorded sequentially in baths containing initially 140 mM NaCl (n=6, open circles) and subsequently 14 mM NaCl (n=4, filled circles). **B.** Whole cell reversal potentials (E_{rev}) in T-Rex cells induced 6 h to express APOL1 G0 as in panel A, measured first in 140 mM NaCl bath (n=6, white bar) and subsequently in 14 mM NaCl bath (n=6, gray bar; two data points overlap at highest value). *, p= 0.02 by paired two-tailed t-test. **C.** Whole cell I-V curve of TRex cells induced 6 h to express APOL1 G1, recorded sequentially in baths containing initially 140 mM NaCl (n=9, open circles) and subsequently 14 mM NaCl (n=8, filled circles). Note different Y axis scales of panels A and C. **D.** Whole cell reversal potentials (E_{rev}) in T-Rex cells induced 6 h to express APOL1 G1 as in panel C, measured first in 140 mM NaCl bath (n=9, white bar) and subsequently in 14 mM NaCl bath (n=9, gray bar). Some data points overlap in both bars. *, p=0.002 by paired two-tailed t-test.

Author Manuscript Author Manuscript Author Manuscript Author Manuscript

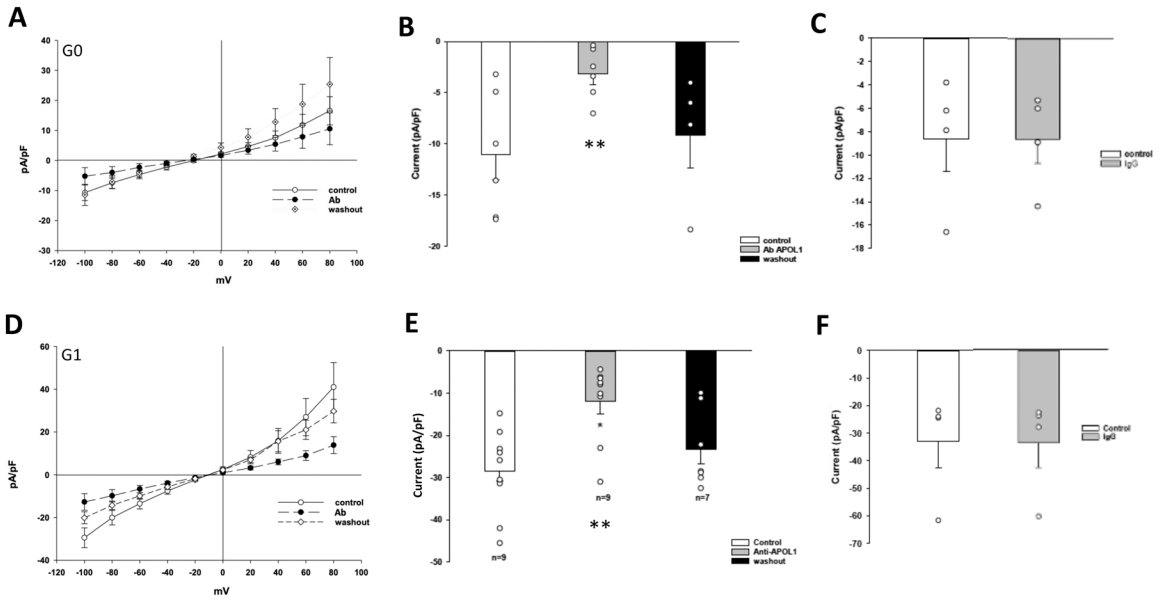

Figure 4. Antibody to APOL1 aa 263–387 partially inhibits whole cell currents in T-Rex cells overexpressing APOL1 G0 or APOL1 G1.

A. Whole cell I-V curves from T-Rex cells induced 6 h to overexpress APOL1 G0, recorded in the initial absence (open circles, n=6) and subsequent presence of rabbit polyclonal antibody to APOL1 C-terminal aa 263–387 (Sigma, 2 μg/ml, filled circles, n=6), followed after 2 min by antibody washout (open dotted diamonds, n=4, recorded after 3 min). **B.** Summarized capacitance-normalized whole cell currents measured at −100 mV in the APOL1 G0-expressing T-Rex cells of panel A, in the absence (control, white bar, n=6), subsequent presence (gray bar, n=6), and after washout of anti-APOL1 C-terminal domain antibody (black bar, n=4). **, p=0.006 vs. control, p=0.037 vs washout; repeated measures ANOVA with Bonferroni post-test. **C.** APOL1 G0 whole cell currents (capacitance-normalized) measured at −100 mV in the absence (white bar) and subsequent presence for 2 min of 2 μg/ml nonspecific rabbit IgG (gray bar, n=4; N.S. for both conditions). **D.** Whole cell I-V curves recorded from T-Rex cells induced 6 h to overexpress APOL1 G1 in the initial absence (open circles) and subsequent presence for 2 min of anti-APOL1 C-terminal domain antibody (2 μg/ml; filled circles), followed by antibody washout for 3 min (open diamonds, n=7 for all conditions). Included in panel E but not D are data from two cells for which patch seals did not survive antibody washout. **E.** Summarized capacitance-normalized APOL1 G1 currents (as in panel D) measured at −100 mV in the initial absence (control, white bar, n=9), subsequent presence of anti-APOL1 antibody (gray bar, n=9), and after antibody washout (black bar, n=7); **, p<0.001 vs control, p=0.008 vs washout; repeated measures ANOVA with Bonferroni post-test. **F.** APOL1 G1-associated whole cell currents (capacitance-normalized) measured at −100 mV in the absence and after 2 min exposure to nonspecific rabbit IgG (2 μg/ml; n=4, N.S. for both conditions).

Author Manuscript Author Manuscript Author Manuscript Author Manuscript

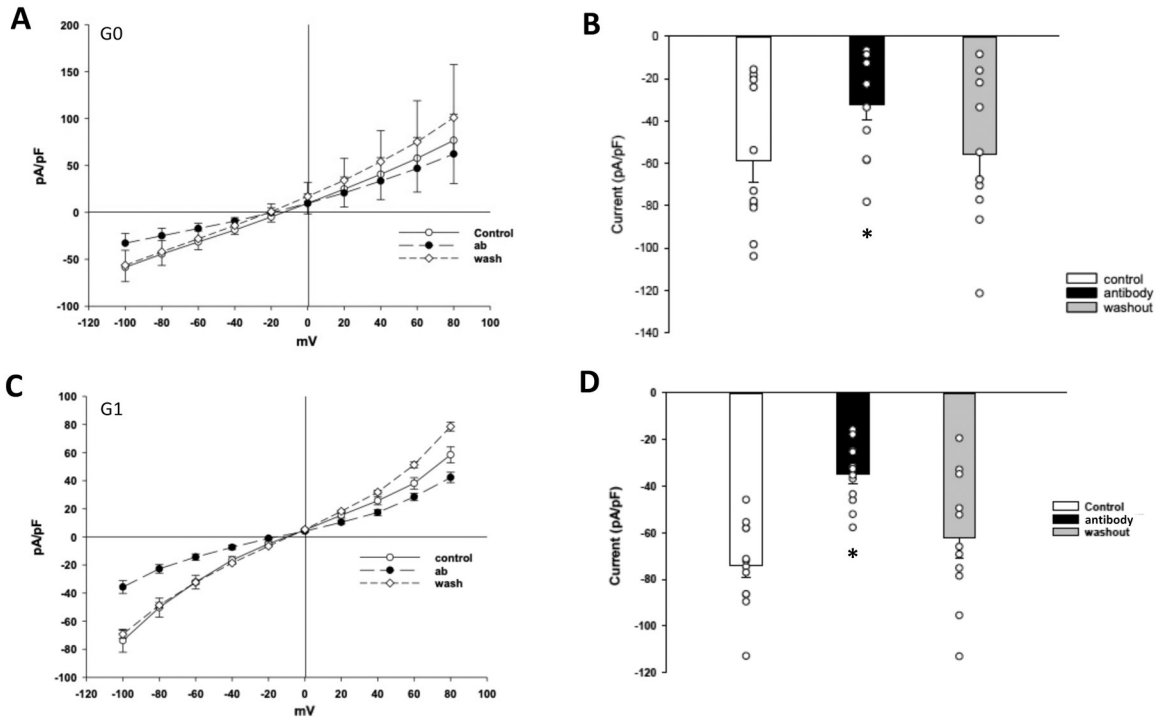

Figure 5. Antibody to APOL1 aa 1–238 partially inhibits whole cell currents in cells overexpressing APOL1 G0 or APOL1 G1.

A. Whole cell I-V curve from HEK-T-Rex cells induced 6 h to overexpress APOL1 G0, recorded before (open circles) and 2 min after bath addition of rabbit polyclonal anti-APOL1 aa 1–238 IgG (Promega, 2 μg/ml, filled circles), and 3 min after subsequent antibody washout (open diamonds). **B.** Summary of capacitance-normalized whole cell currents recorded at −100 mV from the T-Rex cells of panel A overexpressing APOL1 G0 before (control, white bar, n=11) and after bath addition of anti-APOL1 aa 1–238 IgG (2 μg/ml, black bar, n=11) followed by antibody washout (gray bar, n=10). *, $p<0.001$ vs control; $p = 0.002$ vs. washout). Note datapoint overlap in white and black bars. **C.** Whole cell I-V curve from T-Rex cells induced 6 h to overexpress APOL1 G1 before (open circles) and 2 min after bath addition of anti-APOL1 aa 1–238 IgG (filled circles), and 3 min after subsequent antibody washout (open diamonds). **D.** Summary of capacitance-normalized whole cell currents recorded at −100 mV from the T-Rex cells of panel C overexpressing APOL1 G1 in the initial absence (open bar, n=12) and after subsequent presence of anti APOL1 aa 1–238 IgG (black bar, n=12), followed by subsequent antibody washout (gray bar, n=12; data points overlap in all bars). *, $p<0.001$ vs. control, $p<0.011$ vs. washout; repeated measures ANOVA with Bonferroni post-test.

Author Manuscript Author Manuscript Author Manuscript Author Manuscript

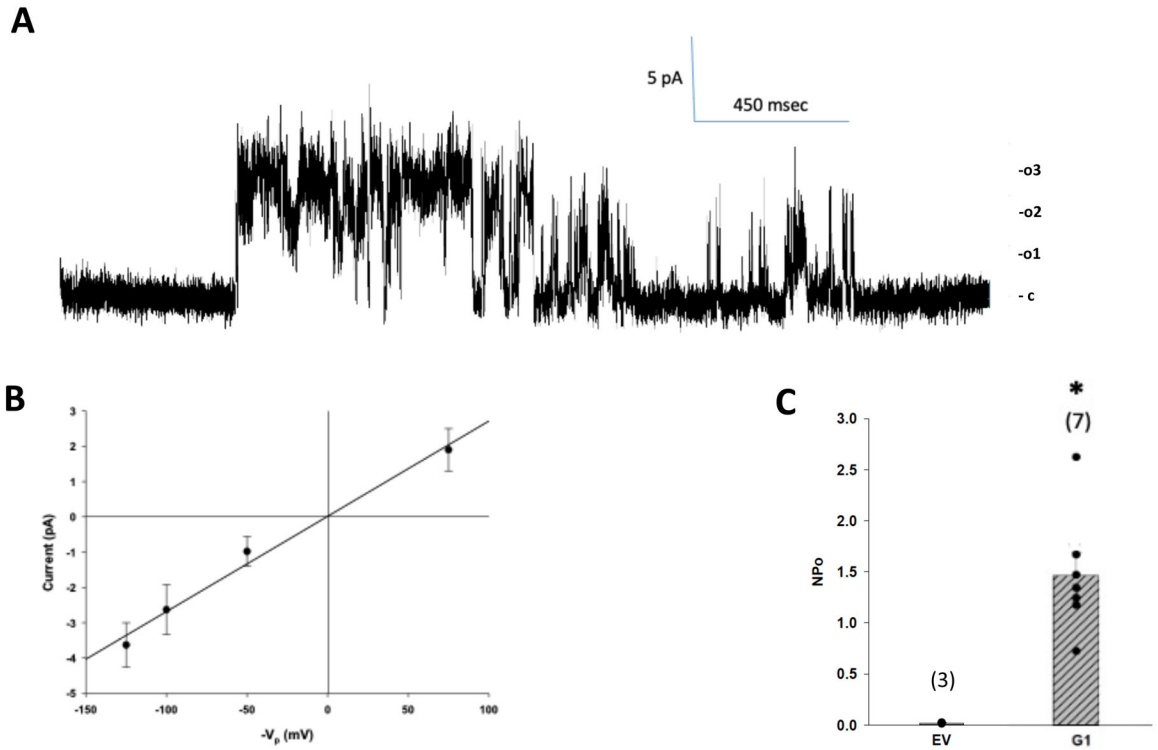

Figure 6. Unitary current associated with APOL1 G1 expression in HEK-293 T-Rex cells.

A. Current trace recorded at Vp = −100 mV in an on-cell patch from a representative T-Rex cell overexpressing APOL1 G1 after 6 h doxycycline treatment. Seal resistance of this patch at the end of recording was 3 GΩ. **B.** Single channel IV curve recorded from an on-cell patch of a different T-Rex cell induced 6 h with doxycycline to express APOL1 G1. Unitary conductance was 27 pS, with NPo of 1.47. **C.** NPo of unitary currents recorded from on-cell patches of T-Rex cells transfected with EV (n=3) or G1 (n=7) after 6 h doxycycline treatment. *, p=0.006 vs EV by unpaired two-way Student t-test.

Author Manuscript Author Manuscript Author Manuscript Author Manuscript

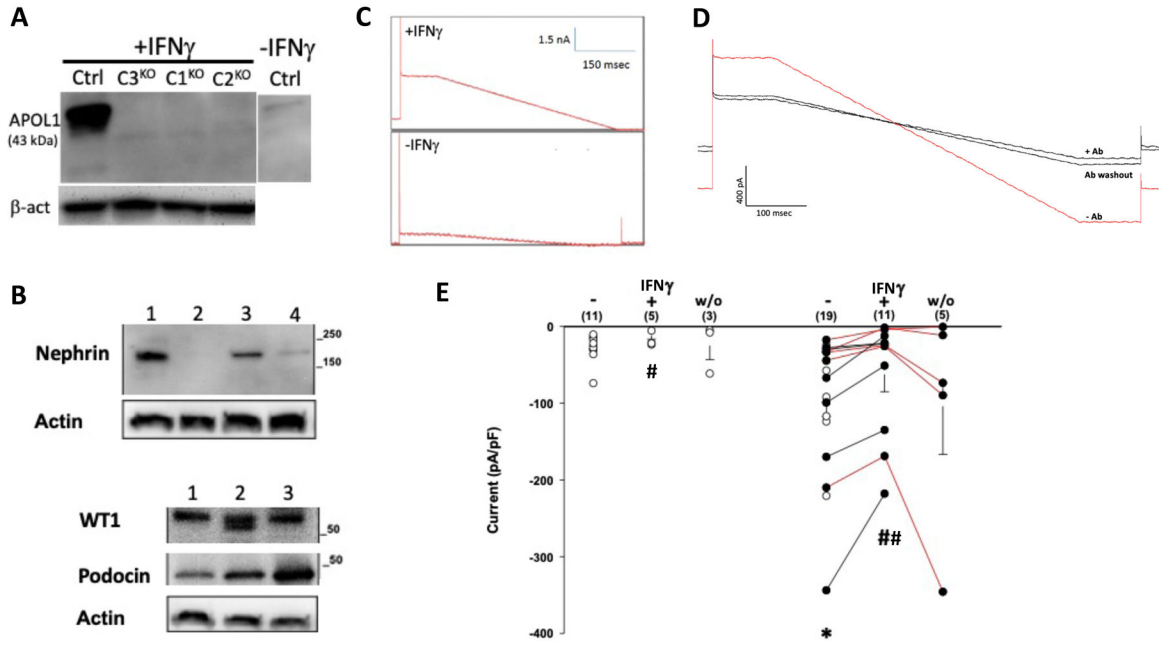

Figure 7. Antibody to APOL1 aa 1–238 partially inhibits whole cell currents of INFγ-induced Celprogen human primary podocytes.

A. Immunoblot detection of APOL1 in podocytes treated in the absence (-INFγ, rightmost lane) or presence of INFγ (Ctrl, leftmost lane). APOL1 is not induced by IFNγ in three clonal populations derived from Celprogen human primary podocytes (C1KO, C2KO, C3KO) in which the *APOL1* gene was subjected to CRISPR-mediated inactivation. β-actin served as loading control. **B.** Preservation of differentiated phenotype in Celprogen podocytes. Upper panels: immunoblot of nephrin in lysates of HEK-293 cells transiently overexpressing nephrin (lane 1), in SV40LgT-immortalized human podocytes (lane 2), in Celprogen primary human podocytes (lane 3) and in podocyte outgrowths from human glomeruli. Lower panels: immunoblots of WT1 and podocin in HEK-293 cells transiently overexpressing WT1 or podocin (lane 1), in SV40LgT-immortalized human podocytes (lane 2) and in Celprogen primary human podocytes (lane 3). β-actin served as loading control for both upper and lower panels. **C.** Whole cell IV curve (linear ramp from +100 (at left) to −100 mV (at right)) recorded from a representative human primary podocyte incubated 18 h in the absence (lower trace) or presence of IFNγ (10 ng/mL, upper trace). **D**. Whole cell IV curve (linear ramp from +100 (at left) to −100 mV (at right), recorded first in the absence (red trace) and then after 2 min in the presence of anti-APOL1 aa 1–238 antibody (black trace +Ab), and finally after 3 min of antibody washout (black trace “washout”). Seal resistances at the end of each period were 9.7 GΩ (-Ab), 8.3 GΩ (+Ab) and 4.0 GΩ (washout). **E.** Capacitance-normalized whole cell currents measured at −60 mV in normal human primary podocytes incubated 24 h in the absence (n=11, left three datasets) or presence of 10 ng/ml IFNγ (n=19, right three datasets); *, $p<0.016$ vs. minus IFNγ. Each cell was recorded first in the absence and then in the subsequent presence of anti-APOL1 N-terminal domain antibody for 2 min (2 μg/ml, +Ab; n=6 −IFNγ and n=11 +IFNγ), followed by 3 min antibody washout (w/o, n=3 −IFNγ and n 5 +IFNγ). Among the 19 IFNγ-pretreated cells, open circles represent cells for which patch seals did not survive the

Author Manuscript Author Manuscript Author Manuscript Author Manuscript

antibody exposure, black circles connected by black lines depict cells for which patch seals did not survive antibody washout, and black circles connected by red lines show cells for which patch seals survived all three recording conditions. #, p= 0.135, vs. −IFNγ before antibody; ##, p=0.008 vs. +IFNγ before antibody; one-way ANOVA on ranks with Dunnett's post-test.

Author Manuscript Author Manuscript Author Manuscript Author Manuscript

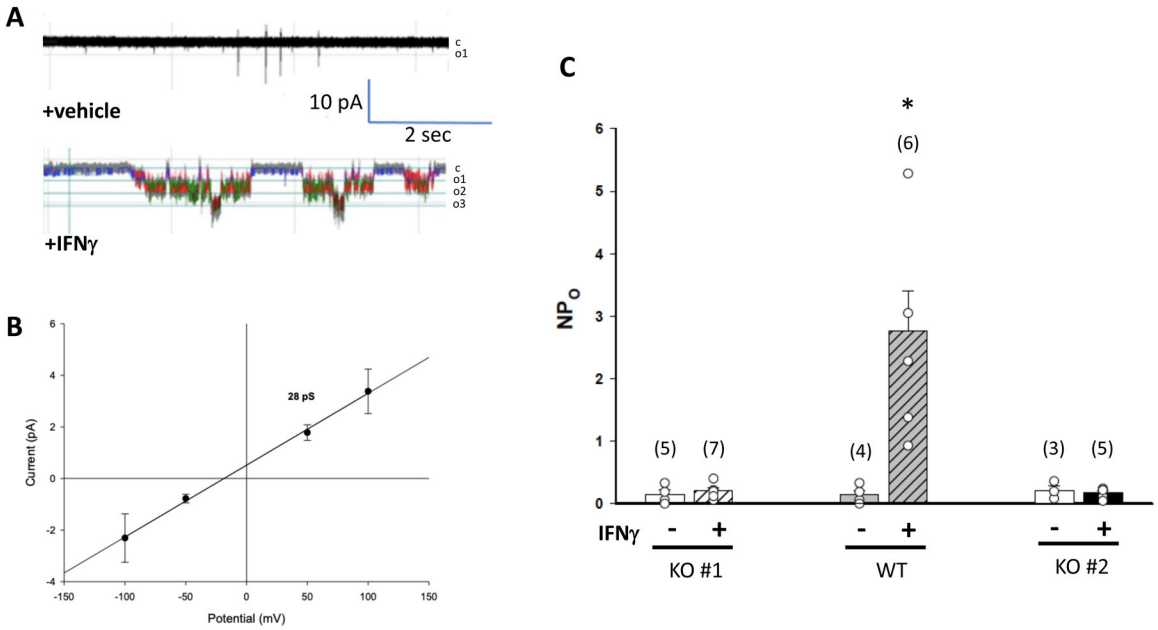

Figure 8. IFNγ-induced single channel activity recorded in on-cell patches of Celprogen human podocytes is abrogated in CRISPR-Cas9 APOL1 knockout cell lines.

A. Representative on-cell current traces measured at −Vp = +50 mV in podocytes previously treated 24 h with vehicle (upper trace) or with IFNγ (10 ng/mL, lower trace). B. I-V curve of the predominant unitary conductance class (28 pS) of on-cell patch currents in a representative IFNγ-treated Celprogen human podocyte. C. NPo of predominant unitary current class in native Celprogen podocytes (WT, middle pair of bars) and in two Celprogen knockout cell lines (KO #1 and KO #2), each treated 24 h in the absence (left unfilled bars of each pair) and presence of IFNγ (right bars of each pair; data points overlap in all bars). Values are means ± s.e.m. for indicated (n). *, $p<0.05$ for WT+IFNγ vs −IFNγ, and for WT+IFNγ vs each KO+IFNγ; unpaired two-way t-tests.

Author Manuscript Author Manuscript Author Manuscript Author Manuscript

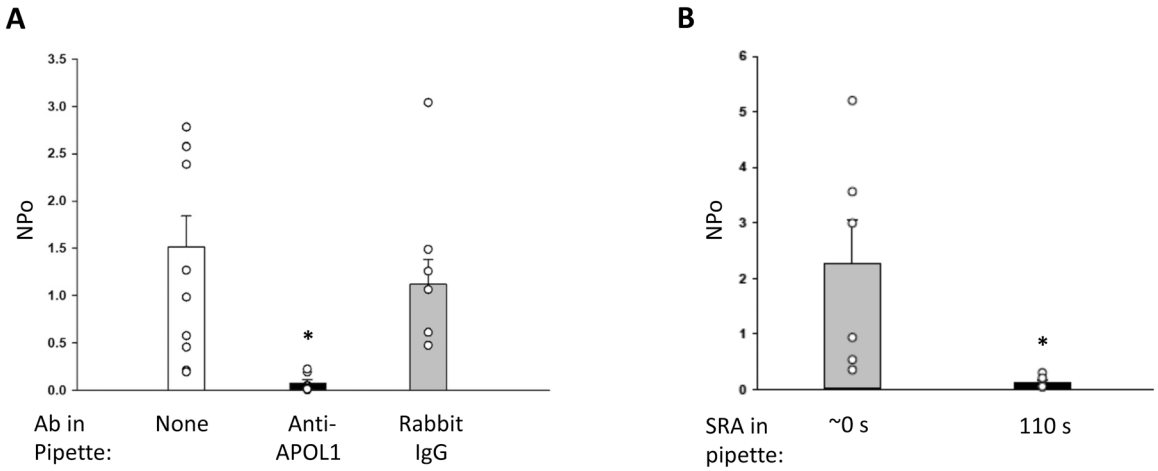

Figure 9. Anti-APOL1 aa 1–238 and a GST fusion protein of *T. brucei rhodesiense* SRA (Serum Response-Associated) aa 24–267 both inhibit APOL1-associated single channel activity in IFNγ-treated primary human podocytes.

A. NPo of unitary currents measured at −Vp = +50 mV in IFNγ-pretreated Celprogen podocytes treated without (n=14, white bar, data points overlap) or with 2 μg/ml anti-APOL1 N-terminal domain antibody (n=7, black bar, data points overlap) or nonspecific rabbit IgG (n=6, gray bar) in the pipette solution. Steady-state values at 2–3 min after achievement of seal. *, p=0.003 vs “none”; unpaired two-tailed t-test. **B.** NPo of unitary currents measured at −Vp = +50 mV in IFNγ-pretreated Celprogen podocytes (n=6) exposed to 3 μM recombinant N-terminal fragment of Serum Response-Associated (SRA) of *Trypanosoma brucei rhodesiense* in the pipette solution, and recorded immediately after establishment of a gigohm seal (gray bar) and ~110 s after seal establishment (black bar; data points overlap). *, p<0.041 vs ~0 sec; unpaired two-tailed t-test. Gigohm resistances were maintained throughout the recording periods.